

Classical disc physics

Giuseppe Lodato^a

^a*Department of Physics and Astronomy, University of Leicester, Leicester, LE1 7RH*

Abstract

I review the basic physical processes that determine the evolution of accretion discs. I first introduce the main properties of discs observed around young stars across the mass spectrum. I then turn to the analysis of the fundamental disc equations, highlighting several subtleties, in some cases rarely discussed in textbooks. I then discuss some classic accretion disc solutions, both steady state and time dependent. I emphasise the description of the outbursting FU Orionis objects, the class of protostellar objects best suited to investigating the accretion process. I discuss in some detail the possible physical mechanisms responsible for transport in accretion discs, with particular emphasis on gravitational instabilities, which are rarely discussed in this context.

1. Introduction

Disc-like or flattened geometries are very common in astrophysics, from the large scale of spiral galaxies down to the small scales of Saturn's rings. In both of these examples, the system is either *collisionless* (in the case of spiral galaxies) or particulate (for Saturn's rings) and cannot be simply described in terms of hydrodynamics. In the last thirty years increasing attention has been given to *fluid* discs, where the dynamically active component is gaseous. Here, dissipative effects, associated with friction or viscosity (a word that will recur very often throughout this Chapter), can significantly alter the dynamics of the disc. Through dissipative effects the fluid elements of the disc can lose their energy or, more fundamentally, their angular momentum, as I describe in more detail below, and can fall towards the bottom of the potential well, hence accreting on to a central gravitating body. Such a system, where a disc feeds a central object through accretion under the effect of viscous forces, is called an **accretion disc**.

Young stars are often surrounded by circumstellar discs, with a very wide range of size, mass, temperature, lifetime, and composition. Each of these properties is a function of stellar mass and evolutionary

stage. Even within a given specific system quantities such as the disc temperature can differ by orders of magnitude between the inner hotter parts of the disc and the outer, colder ones. I give a brief account of the main properties of discs around young stars in Section 3 below.

Circumstellar discs are an essential component in the context of star formation. First, they play an important *dynamical* role, since it is through the disc that the central young star accretes most of its mass. As discussed below, the angular momentum of a molecular cloud core, where stars are born, is orders of magnitude larger than the angular momentum of a star. To form the star, one needs to find a way to remove the excess angular momentum and let the matter fall into the centre. An accretion disc provides just the mechanism to accomplish this.

A second very important role played by circumstellar discs is as the site of planet formation. This idea is centuries old, and dates back from the arguments by Kant and Laplace, who noted that all the planets of our own Solar System are almost coplanar and orbit the Sun in the same direction, thus suggesting a common origin within a rotating disc. Events in the disc, such as processing of various gaseous species and the growth of dust grains, there-

fore play an important *chemical* role. A detailed description of the issues related to planetary formation is provided in the Chapters by Alexander and Klahr within this volume.

The focus of this Chapter is on the basic dynamics of accretion discs. This is an essential first step needed to embark on the discussion of the more complex phenomena associated with planet formation and also to understand and make sense of the observations that will become available in the future at progressively higher angular resolution. Several excellent reviews and textbooks have been written over the years on the dynamics of accretion discs. The basic physical principles underlying the evolution of such systems have been described in Pringle (1981) and in Frank et al. (2002). A comprehensive review of the importance and of the dynamics of discs around young stars is provided by Hartmann (1998), while planet formation has been recently reviewed by Armitage (2007). A thorough description of the transport properties of discs, and of the magnetohydrodynamics (MHD) instabilities responsible for them has been recently provided by Balbus and Hawley (1998) and Balbus (2003).

These references provide an extensive background on the subject. Here, I will provide a step-by-step approach to the subject, from a theoretical perspective. I introduce the main disc properties in Section 3 and derive in Section 4 the basic equations that determine the disc evolution from first principles (i.e., from the Navier-Stokes equations, describing the motion of a viscous fluid). In Section 5 I discuss the energetics of accretion discs. After a brief description of the most important timescales determining the disc evolution (Section 6), I discuss in some detail FU Orionis objects and the possible instabilities that determine their outbursts (Section 7). Finally, I discuss the major issue in accretion disc physics, that is, what process is ultimately responsible for accretion and dissipation, or, in other words, what determines the disc *viscosity* (Section 8). This is commonly attributed to the development of magnetohydrodynamical instabilities, which are treated in more detail in the Chapter by Ferreira in this volume. However, as discussed below, circumstellar discs may be too cold for MHD instabilities to operate and we may have to resort to other processes, such as gravitational instabilities. This latter topic is more rarely discussed and reviewed (and only in the context of the so-called disc fragmentation scenario for planet formation, see Durisen et al. 2007), so I will spend some time discussing it (Sec-

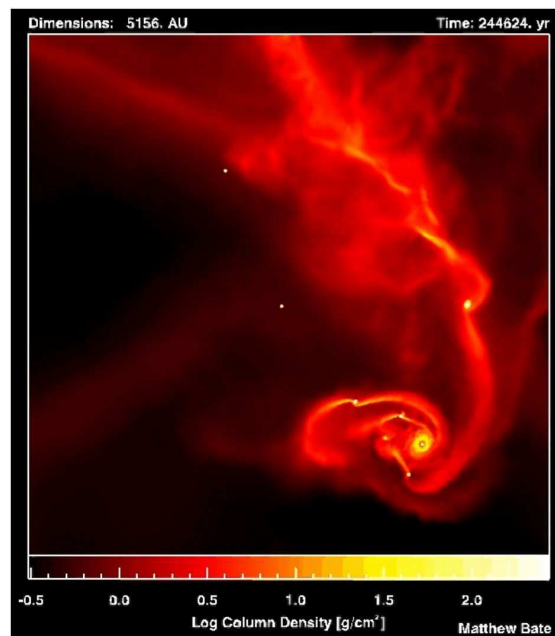


Fig. 1. Snapshot of a numerical Smoothed Particles Hydrodynamics simulation of the formation of a stellar cluster. A few protostars are visible as bright spots in the image, while the colour scale indicates gas density. A large disc is visible on the bottom right corner, while another smaller one is forming above it. Image from M. Bate.

tion 8.7). Finally, I finish by pointing out some of the interesting new directions still worth exploring in the theoretical understanding of disc evolution.

2. Why discs?

The formation of discs is related to the angular momentum content of the molecular cloud core within which stars form. Without rotation, the gas in the core could in principle freely collapse towards the centre, forming a relatively compact protostar. However, even a small amount of angular momentum prevents such radial collapse, allowing the gas to sink down only to a minimum distance from the centre. Observations of molecular cloud cores typically yield angular velocities of the order of $\Omega_{\text{core}} \approx 10^{-14} - 10^{-13} \text{sec}^{-1}$. However we cannot simply take these values to represent angular velocities in the disc. Angular momentum conservation forces the gas to rotate faster as it collapses. So, what is the typical angular momentum per unit mass of a molecular cloud core? A simple estimate of a molecular cloud core mass can be obtained by asking what is the mass for which thermal pressure is just enough to counterbalance gravity and prevent collapse. Equivalently,

we can ask what is the maximum size λ_J for which the sound crossing time $t_{sc} \sim \lambda_J/c_s$ is comparable to the free-fall timescale $t_{ff} \sim (G\rho)^{-1/2}$, where ρ is the gas density. This typical lengthscale is called the “Jeans length” and its exact definition is:

$$\lambda_J = \frac{2\pi c_s}{\sqrt{4\pi G\rho}}. \quad (1)$$

The mass associated with this lengthscale is called the “Jeans mass” and is given by:

$$M_J = \rho\lambda_J^3 \sim \frac{\pi^{3/2}}{G^{3/2}} \frac{c_s^3}{\rho^{1/2}}. \quad (2)$$

The isothermal sound speed for the gas is related to the temperature by $c_s^2 = kT/\mu m_p$, where m_p is the proton mass and $\mu \approx 2.3$ is the mean molecular weight. For a typical temperature $T \approx 10\text{K}$ for molecular cloud cores, we find that a core whose Jeans mass is of the order of one solar mass, $M_J \approx M_\odot$, has a Jeans length of order 0.1 pc. Interestingly, this is just about the observed size of typical molecular cloud cores (McKee & Ostriker, 2007). The specific angular momentum of the gas in the core can therefore be estimated through:

$$j \approx \Omega_{\text{core}}\lambda_J^2 \approx 10^{21} - 10^{22} \text{cm}^2/\text{sec}, \quad (3)$$

Fluid elements falling towards the centre will initially be in eccentric orbits around the central protostar, but rapidly lose energy through shocks and dissipation and settle down in the minimum energy orbit for a given angular momentum, i.e. a circular orbit. We can ask at what distance from the star the gas will be in centrifugal equilibrium. Thus we match the specific angular momentum of the infalling material to that appropriate for a Keplerian orbit, i.e.

$$j_K = \sqrt{GMR}, \quad (4)$$

at a distance R from a star of mass M . We see that the gas adopts Keplerian orbits around the protostar at a distance

$$R_{\text{disc}} = \frac{j^2}{GM} \approx 10^2 - 10^4 \text{AU}, \quad (5)$$

where we assumed $M \approx 1M_\odot$ and estimated j from equation (3) above. This is clearly much larger than the size of a star, so the gas needs to redistribute the angular momentum in order to accrete further to the centre.

To summarize, we have seen that the collapse of a rotating gaseous cloud leads to the formation of a flattened structure (a disc) of typical size $R_{\text{disc}} \gtrsim$

10^2 AU. Once landed on the disc, in order to further accrete onto the forming protostar, the gas has then to find a way to get rid of its angular momentum. The way to accomplish that is provided by the accretion disc.

In reality, the dynamics that leads to the formation of a stellar cluster can be much more complex than the simple picture for the formation of an isolated star described above, as shown by the simulations performed by Bate et al. (2003) (see Fig. 1), which include the important effects of dynamical interactions between the forming stars and the possibility of binary formation. Additionally, the presence of magnetic fields can also affect the process of star formation (Machida et al., 2004; Price & Bate, 2007). Even in this more complex environment, however, the basic physics described above (which is essentially based on angular momentum conservation) still work. Circumstellar discs are the natural outcome also in this case.

3. Main properties of circumstellar discs

Circumstellar discs are found around stars of very different mass, from brown dwarfs (with stellar mass $M < 0.08M_\odot$) up to massive stars (with stellar mass $M > 8M_\odot$). This is reflected in the large range of observed disc properties, which generally span several orders of magnitude and are a function of both stellar mass and evolutionary stage. In general, the most detailed information available is for discs around young solar mass objects.

Typically young stellar objects are classified according to their infrared spectral energy distribution (Lada and Wilking, 1984), and this classification is usually interpreted as an evolutionary sequence (Adams et al., 1988). Class 0 and Class I objects have a spectrum that rises toward longer wavelengths, indicating the presence of a large amount of cold material surrounding the star. Such objects are probably the youngest ones, and are still embedded in an optically thick envelope that dominates the emission, with some contribution being provided also by the disc (Adams et al., 1988; Kenyon et al., 1993; Eisner et al., 2005). Class II objects have a generally declining spectrum, but still show a substantial excess emission with respect to a standard stellar photosphere. The emission in this case is thought to be mostly due to the disc, which can be actively accreting (and therefore self-luminous, see below) or simply heated by the stellar radiation, or most proba-

bly a combination of the two. Stars in this Class are also often called Classical T Tauri stars. Class III objects (also sometimes referred to as weak line T Tauri stars) have only small excess emission above a stellar photosphere and most of the circumstellar material has been cleared out by this stage. Additionally, an important small class of objects are the so-called FU Orionis objects (that will be discussed in more detail below), that are thought to be Class I or Class II objects undergoing strong outbursts, due to a sudden increase of their accretion rate.

3.1. *Disc masses*

Circumstellar discs are essentially composed of gas and dust. The gaseous component dominates the mass of the system, with the dust only contributing to roughly 1-2% of the total disc mass. The dynamics of the disc is thus almost completely dominated by the gas. On the other hand, the dust component is very important, as it dominates the opacity and therefore the emission properties of the disc, as well as the ionisation state of the gas, and hence the coupling to the magnetic field. This puts us in a relatively uncomfortable position, as most of the mass of the disc is essentially invisible to us.

Disc masses are generally estimated from sub-mm emission, since at these wavelengths dust emission is usually optically thin and we can thus easily convert the observed flux into a mass, if we know the dust opacity (Beckwith et al., 1990). Recent surveys of discs around solar mass stars in the Taurus-Auriga complex (Andrews and Williams, 2005) indicate disc masses between $10^{-4}M_{\odot}$ and $10^{-1}M_{\odot}$, with a median value of $5 \cdot 10^{-3}M_{\odot}$. Andrews and Williams (2007) report the results for a smaller sample (possibly biased to larger masses) for which the median mass is one order of magnitude larger and in a few cases discs as massive as $0.2M_{\odot}$ have been found. Similar values are also reported for the Orion region, where in a few cases masses as large as $0.4M_{\odot}$ have also been reported (Eisner and Carpenter, 2006). Since the stellar mass for these samples ranges between 0.1 and $1M_{\odot}$, the mass ratios between the disc and the star is between 10^{-3} and a few times 10^{-1} .

It should be noted, however, that such measurements suffer from very large systematic errors, mostly due to uncertainties in the dust opacity. Indeed, in many cases there is evidence for relatively evolved dust grains, so that the dust size distribution can be significantly different than in the

interstellar medium (Testi et al., 2001; Natta et al., 2004). If dust grains have evolved to relatively large sizes, their opacity would be reduced and the inferred disc mass would correspondingly increase. It is therefore likely that most of the above estimates are actually underestimating the real disc masses (Hartmann et al., 2006).

If we consider discs in the brown dwarf range, disc mass measurements are only available for a limited number of objects (Scholz et al., 2006), with upper limits at the level of a few Jupiter masses, corresponding to a few percent of the (sub)-stellar mass.

Moving up to high mass stars, the situation appears to be slightly different. While discs have been detected only in a limited number of cases, the inferred disc mass appears to be rather high, amounting to a sizeable fraction of the central object mass (for a recent review, see Cesaroni et al. 2007).

3.2. *Disc sizes and temperature*

In order to constrain the disc size we need to resolve it. This is usually done with sub-mm interferometry (Dutrey et al., 1996). Recent observations in Taurus (Andrews and Williams, 2007) indicate sizes of a few hundreds up to one thousand AU, roughly consistent with the theoretical estimates made in the previous Section.

For discs around high-mass stars the situation is more complicated. While often rotating structures are observed around young O stars, with sizes up to 10^5 AU, such structures are most probably not in centrifugal equilibrium (see below), given the large dynamical timescales involved. On the other hand, smaller size discs ($\sim 10^4$ AU, that might be in centrifugal balance) are often observed around B stars (Cesaroni et al., 2007).

Disc sizes in the brown dwarf regime are not very well determined, but they often appear to be more extended than a few tens of AU (Scholz et al., 2006).

The disc temperature varies considerably, even within individual discs. In the inner regions, the temperature can reach a few thousand K, while in the outer disc, it can drop down to a few tens of K. The disc temperature is important since, as will be described below, it sets the typical scale for the disc thickness H . Typically, circumstellar discs have aspect ratios $H/R \sim 0.1$, where R is the cylindrical radius in the disc.

3.3. Accretion rates

Accretion rates \dot{M} are generally measured either from the strength of emission lines emitted as the gas reaches the star in the so called ‘magneto-spheric accretion’ model, when the innermost parts of the disc are truncated by the stellar magnetic field, and the gas falls almost freely onto the star along magnetic field lines, or from the veiling of photospheric lines due to accretion shocks (Gullbring et al., 1998, 2000).

It should be noted here that these measurements refer to the accretion rate onto the star, which does not necessarily correspond to the accretion rate at larger radii, if significant sinks of matter are present, such as a disc wind (which is generally very small) or, more likely, as a massive planet, whose presence might act like a dam for the accretion flow.

In any case, typical values range from $10^{-11}M_{\odot}/\text{yr}$ for brown dwarfs, to $10^{-9} - 10^{-7}M_{\odot}/\text{yr}$ for T Tauri stars, up to $10^{-5}M_{\odot}/\text{yr}$ for discs around massive stars. Recently, attention has been put to the fact that the accretion rates appear to scale almost quadratically with the stellar mass (Natta et al., 2004). While this scaling might bear some relation to the initial distribution of stellar properties (Alexander and Armitage, 2006), it is not yet clear how much this result is affected by observational biases (Clarke and Pringle, 2006).

Occasionally, discs around solar mass stars are observed to suddenly increase their accretion luminosity, and to produce large outbursts (called FU Orionis outbursts), during which the accretion rate can be as large as a few times $10^{-4}M_{\odot}/\text{yr}$ (Hartmann and Kenyon, 1996). FU Orionis outbursts will be discussed in more detail in Section 7 below.

3.4. Disc lifetimes

Disc lifetimes are generally obtained by comparing the fraction of stars which show an infrared excess (taken as an indication of the presence of a disc) in young stellar clusters of different ages (Haisch et al., 2001; Sicilia-Aguilar et al., 2006). Typical numbers are of the order of a few (up to 10) million years.

4. Accretion disc dynamics

4.1. The thin disc approximation

Accretion discs are often assumed to be thin. This means that the typical length in the vertical direction, the disc thickness H , is much smaller than the radial distance R . We have seen above that this condition generally holds for circumstellar discs, where $H/R \approx 0.1$.

The thin disc condition allows us to treat the disc, to a first approximation, as infinitesimally thin, and to introduce a *small quantity*, the aspect ratio $H/R \ll 1$. This implies that most of the equations we are going to use can be integrated in the vertical direction, and rather than dealing with quantities *per unit volume* (such as the density ρ), we will deal instead with quantities *per unit surface* (such as the surface density Σ). When “volume” quantities are needed (for example the viscosity ν), these will generally be understood as vertically averaged.

The fundamental ordering of lengthscales $H/R \ll 1$ is also related to a similar ordering in terms of velocities. Indeed, one can show (see section 4.4) that this ordering is equivalent to requiring that the sound speed c_s is much smaller than the rotational velocity v_{ϕ} . It is useful to anticipate another important relation between the relevant velocities, derived by requiring that accretion takes place on a long timescale. This condition implies that the radial velocity v_R should be smaller than both the sound speed and the rotational speed. We can therefore summarize these relations as

$$v_R \ll c_s \ll v_{\phi}. \quad (6)$$

4.2. Gas dynamics of viscous discs

The evolution of accretion discs can be described by the basic equations of viscous fluid dynamics: the continuity equation and Navier-Stokes equations. Given the geometry of the problem, we adopt cylindrical polar coordinates centred on the star and we assume that to first order the disc is axisymmetric, so that no quantity depend on the azimuthal angle ϕ .

Consider then a disc with surface density $\Sigma(R, t)$. In cylindrical coordinates, the continuity equation (integrated in the vertical direction following the thin disc approximation) reads

$$\frac{\partial \Sigma}{\partial t} + \frac{1}{R} \frac{\partial}{\partial R} (R \Sigma v_R) = 0. \quad (7)$$

To determine the velocity \mathbf{v} , we use the momentum equation including viscous forces, i.e. the Navier-Stokes equation. This reads:

$$\frac{\partial \mathbf{v}}{\partial t} + (\mathbf{v} \cdot \nabla) \mathbf{v} = -\frac{1}{\rho} (\nabla P - \nabla \cdot \sigma) - \nabla \Phi. \quad (8)$$

The above equation is simply a statement of Newton's second law. The left hand side is the acceleration, including the second term, which describes the momentum convected into the fluid by velocity gradients¹. On the right-hand side, we find the various forces acting on the fluid. First of all, we have the term describing pressure forces, where P is the pressure and ρ is the density. We then have gravity, represented by the last term on the right-hand side, where Φ is the gravitational potential. In most cases, gravity is dominated by the central star, with mass M , so that the potential is simply given by:

$$\Phi = -\frac{GM}{r}, \quad (9)$$

where here r is the spherical radius. The gravitational force is obviously directed in the radial direction, and is given by:

$$-\nabla \Phi = -\frac{GM}{r^2} \hat{\mathbf{r}}. \quad (10)$$

However, in some cases (see Section 8.7) the disc could be massive enough to make a non-negligible contribution to Φ . The calculation of the gravitational potential in this case is a bit more complex, but under some conditions it can be easily accounted for (Bertin and Lodato, 1999).

Finally, the second term on the right hand side in equation (8) contains the stress tensor σ and describes the effect of viscous forces. This term plays a very important role in accretion disc dynamics. The nature of the disc viscosity and of the stress tensor σ will be discussed at length below. In its simplest form, it can be assumed to be given by classical shear viscosity, so that the only non vanishing component of σ in a circular shearing flow is the $R\phi$ component, proportional to the rate of strain $R\Omega'$ (where $\Omega' = d\Omega/dR$):

$$\sigma_{R\phi} = \rho \nu R \frac{d\Omega}{dR}, \quad (11)$$

¹ The two terms on the left-hand side are collectively called the Lagrangian derivative of the velocity.

where $\Omega = v_\phi/R$ is the angular velocity and we have introduced the kinematic viscosity ν , which has the dimensions of length times velocity. Equation (8) has three components in the radial, vertical and azimuthal directions, respectively, and each one defines some important properties of accretion discs. In the following three sections we will examine in turn each of these three equations.

4.3. Radial equilibrium: centrifugal balance

Let us first consider the radial component of equation (8). Here, the ordering of velocities described above turns out to be particularly useful. In particular, on the left-hand side, the first term, $\partial v_R/\partial t$, is negligible with respect to the second term, which (when using the appropriate expression for the differential operators in cylindrical coordinates) gives rise to the centrifugal term $-v_\phi^2/R$. On the right-hand side, the viscous term vanishes and the pressure term can be obtained using the equation of state. If the gas is barotropic (i.e. if pressure only depends on density), the sound speed is simply defined as

$$c_s^2 = \frac{dP}{d\rho}. \quad (12)$$

We then have

$$\frac{1}{\rho} \frac{\partial P}{\partial R} = \frac{c_s^2}{\rho} \frac{\partial \rho}{\partial R} \sim \frac{c_s^2}{R}. \quad (13)$$

Since $c_s \ll v_\phi$, also this term is second order with respect to the leading term. The only term on the right hand side able to balance the centrifugal force is therefore the radial component of the gravitational force (see eq. (10)). We then have, to first order

$$\frac{v_\phi^2}{R} \simeq \frac{d\Phi}{dR} = \frac{GM}{R^2}, \quad (14)$$

which express the condition of centrifugal balance, where we have considered the case where the disc self-gravity does not contribute to Φ , and where we have also used the fact that for a thin disc $r \sim R$. The rotational velocity is then

$$v_\phi^2 = v_K^2 = \frac{GM}{R}, \quad (15)$$

and the angular velocity $\Omega_K = v_K/R$ is

$$\Omega_K^2 = \frac{GM}{R^3}. \quad (16)$$

The two conditions above are simply a restatement of Kepler's third law, and therefore discs that obey these relations are called ‘‘Keplerian’’ discs. Note that a Keplerian disc is strongly shearing in the radial direction, since Ω is a relatively strong decreasing function of R . On the other hand, the angular momentum per unit mass in the disc is

$$v_K R = \sqrt{GM R}, \quad (17)$$

and is thus an increasing function of R .

The above derivation is only valid to first approximation, since we have neglected the pressure forces in the radial direction. This is generally a good approximation, but in some cases the small departures from Keplerian rotation due to pressure effects might play an important role. In particular, this is the case when one considers the dynamics of small solid bodies within the disc (a very important component involved in the process of planet formation, as discussed in the Chapter by Alexander of the present book). The solids are not subject to pressure and would thus move on exactly Keplerian orbits. This therefore generates a small velocity difference with respect to the gas, which in turn determines a very fast migration of the solid (Weidenschilling, 1977; Rice et al., 2004, 2006). Let us then calculate this correction. The radial equation of motion, including pressure terms is²

$$\frac{v_\phi^2}{R} = \frac{1}{\rho} \frac{\partial P}{\partial R} + \frac{GM}{R^2}. \quad (18)$$

If we introduce the sound speed c_s and make the simple assumption that the density ρ has a power law dependence on radius, with power law index $-\beta$ (so that $\rho \propto R^{-\beta}$), we obtain

$$v_\phi = \sqrt{\frac{GM}{R}} \left[1 - \beta \left(\frac{c_s}{v_K} \right)^2 \right]^{1/2}. \quad (19)$$

In cases where the disc is hot, in the sense that the sound speed is non negligible with respect to the Keplerian velocity, there can be sizeable deviations from Keplerian rotation. This can happen, for example, in the hot boundary layers close to the surface of the star, if the disc is not truncated by the magnetic field of the star.

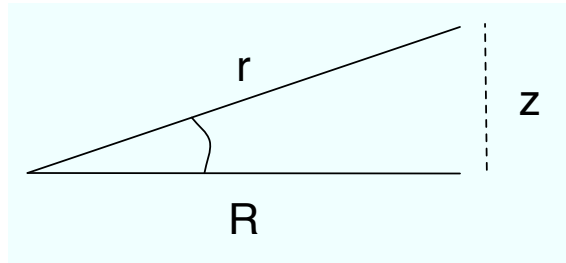


Fig. 2. Geometry involved in the calculation of the disc vertical structure.

4.4. Vertical structure: hydrostatic equilibrium

We now consider the vertical component of equation (8). Here, since the velocity in the vertical direction is very small (the disc being confined to the equatorial plane), we can neglect the left-hand side of the equation altogether. The viscous force vanishes as well, since the only non-zero component of the stress is in the $R\phi$ direction. We are therefore left with just two terms to balance: gravitational force and pressure force in the vertical direction. Such a situation, where gravity is balanced by pressure, is called ‘‘hydrostatic balance’’. The equation reads

$$\frac{1}{\rho} \frac{\partial P}{\partial z} = -\frac{d\Phi}{dz}. \quad (20)$$

We again first consider the case of non-self-gravitating discs. In this case, the vertical component of gravity is simply

$$-\frac{GM}{r^2} \hat{z} \sim -\frac{GM}{r^2} \tan \delta \sim -\frac{GM}{R^2} \frac{z}{R}, \quad (21)$$

where r is the spherical radius and δ is the longitudinal angle above the disc (see geometry in Fig. 2) and the approximation is valid for small z . We can then rewrite Equation (20) as

$$\frac{c_s^2}{\rho} \frac{\partial \rho}{\partial z} = -\frac{GMz}{R^3} = -\Omega_K^2 z. \quad (22)$$

The solution to this equation is straightforward if the sound speed is independent of z . The vertical density profile in this case turns out to be a Gaussian

$$\rho(z) = \rho_0 \exp \left[-\frac{\Omega_K^2 z^2}{2c_s^2} \right] = \rho_0 \exp \left[-\frac{z^2}{2H^2} \right], \quad (23)$$

where ρ_0 is the midplane density and we have introduced the thickness H such that

² Note that this effect is similar to the so-called ‘asymmetric drift’ discussed in the context of galaxy dynamics.

$$H = \frac{c_s}{\Omega_K}. \quad (24)$$

Note the simple relation between the thickness, the sound speed and the angular velocity. The disc aspect ratio is then

$$\frac{H}{R} = \frac{c_s}{v_K}, \quad (25)$$

which then demonstrates, as anticipated above, that requiring that the disc be thin is equivalent to requiring that the disc rotation is highly supersonic, $v_K \gg c_s$. This is generally satisfied for most of the radial extent of the disc, except possibly very close to central star, in cases where the accretion rate is particularly large, such as in the case of FU Orionis objects (Popham et al., 1993).

The above discussion shows the close relationship between the disc thickness and its temperature $T \propto c_s^2$. The physical origin of this relation is easily understood: due to thermal pressure, the disc tends to expand in the vertical direction, counteracting gravity, and the hotter the disc, the stronger this tendency is. In order to obtain the vertical structure of the disc at different radii, we thus need to know how does the temperature vary with radius. This can vary significantly between different objects and in particular it strongly depends on whether the disc is “active” (that is, heated by the accretion process), or “passive”, (that is, heated by the central star). We postpone a more detailed discussion of these regimes to section 5.2.

Before moving on to the analysis of the last component of equation (8), let us see what happens when the disc self-gravity is non-negligible. We first consider the extreme case where the vertical gravitational field is dominated by self-gravity. In this case, we simply have to replace the gravitational force on the right hand side of equation (22) with the force produced by a slab of gas with surface density Σ . This is given by:

$$F_{\text{sg}} = -2\pi G\Sigma. \quad (26)$$

The solution of the hydrostatic balance in this case is more difficult but can be done analytically (Spitzer, 1942). The density profile in this case is not Gaussian, but is given by:

$$\rho(z) = \rho_0 \frac{1}{\cosh^2(z/H_{\text{sg}})}, \quad (27)$$

where the thickness in the self-gravitating case is:

$$H_{\text{sg}} = \frac{c_s^2}{\pi G\Sigma}. \quad (28)$$

Note that both the radial and the vertical component of the gravitational field produced by the disc itself are of the order of $\pi G\Sigma \sim GM_{\text{disc}}/R^2$. Therefore, in order for the self-gravity to produce some modifications to the Keplerian velocity profile, the disc mass has to be a sizable fraction of the central object (which is generally unlikely). On the other hand, the vertical component of the star’s gravitational field is smaller than the radial by a factor H/R (cf. Eq. (21)) and thus the vertical structure of the disc is affected by self-gravity already when the disc mass is of the order of:

$$\frac{M_{\text{disc}}}{M} \approx \frac{H}{R} \ll 1. \quad (29)$$

Further discussions on this issue and a calculation of the disc thickness in the mixed case when both the star and the disc contribute to the vertical gravitational field can be found in Bertin and Lodato (1999).

4.5. Angular momentum conservation

We finally discuss the last component of Navier-Stokes equation, in which the viscous term plays an important role. By the assumption of axisymmetry, the pressure and gravitational forces do not give any contribution in this direction. Let us then write the ϕ component of Equation (8), opportunely integrated in the vertical direction:

$$\Sigma \left(\frac{\partial v_\phi}{\partial t} + \frac{v_R v_\phi}{R} + v_R \frac{\partial v_\phi}{\partial R} \right) = \frac{1}{R^2} \frac{\partial}{\partial R} (R^2 T_{R\phi}), \quad (30)$$

where $T_{R\phi}$ is the vertical integral of the relevant component of the stress tensor, and the last two terms on the left hand side are the obtained from writing the differential operators in cylindrical coordinates. Combining the above equation with continuity equation (7) and after a little algebra, it is possible to rewrite it in a more transparent form:

$$\frac{\partial}{\partial t} (\Sigma R v_\phi) + \frac{1}{R} \frac{\partial}{\partial R} (R v_R \Sigma R v_\phi) = \frac{1}{R} \frac{\partial}{\partial R} (R^2 T_{R\phi}). \quad (31)$$

The physical interpretation of the above expression is readily apparent. The left hand side is the Lagrangian derivative of the angular momentum per unit mass $\Sigma R v_\phi$, while the right hand side is the torque exerted by viscous forces.

A very important case occurs when the rotation curve is Keplerian and the stress tensor is the simple viscous stress tensor. In this case, we have $v_\phi = \sqrt{GM/R}$, $\Omega = v_\phi/R = \sqrt{GM/R^3}$, $R v_\phi = \sqrt{GM R}$.

The vertically integrated stress tensor is given by (cf. Eq. (11)):

$$T_{R\phi} = \nu \Sigma R \Omega'. \quad (32)$$

Then equation (31) takes the form:

$$\frac{\partial}{\partial t}(\Sigma R^2 \Omega) + \frac{1}{R} \frac{\partial}{\partial R}(\Sigma v_R R^3 \Omega) = \frac{1}{R} \frac{\partial}{\partial R}(\nu \Sigma R^3 \Omega'). \quad (33)$$

With the help of the continuity equation (Eq. (7)), we can obtain the radial velocity in this case from equation (33):

$$v_R = \frac{\frac{\partial}{\partial R}(\nu \Sigma R^3 \Omega')}{R \Sigma \frac{\partial}{\partial R}(R v_\phi)} = -\frac{3}{\Sigma R^{1/2}} \frac{\partial}{\partial R}(\nu \Sigma R^{1/2}), \quad (34)$$

which can be inserted back in equation (7) to finally give:

$$\frac{\partial \Sigma}{\partial t} = \frac{3}{R} \frac{\partial}{\partial R} \left[R^{1/2} \frac{\partial}{\partial R} (\nu \Sigma R^{1/2}) \right]. \quad (35)$$

The equation above is one of the key equations in accretion disc theory. It is a diffusion equation for the surface density Σ , whose temporal evolution is determined only by the kinematic viscosity ν . This clearly emphasises the extremely important role of viscosity (or of whatever process is providing a non-negligible stress tensor) in accretion disc theory, since it ultimately is the quantity that determines the evolution of the disc density.

4.5.1. On the direction of angular momentum flux

In the next sections we will provide some examples of solutions of Equation (35) both in the time-dependent case, and in a steady state. However, before moving on, it is instructive to point out some subtleties associated with the derivation above. As it is apparent from Eqs. (31) and (32) above, the internal viscous torque (that is, the flux of angular momentum transported by viscosity across an annulus of the disc) is proportional to the rate of shear $R\Omega'$ and in particular, the outward flux of angular momentum across an annulus at radius R (i.e. the torque of an inner annulus on an outer one) is given by:

$$G(R) = -2\pi R^2 T_{R\phi} = -2\pi \nu \Sigma R^3 \Omega'. \quad (36)$$

This result is intuitively correct: if the disc is in solid body rotation, with $\Omega = \text{const.}$, obviously shear viscosity does not transport any angular momentum and $G(R)$ vanishes. Also note that when, as usually occurs, for example in Keplerian discs, $\Omega(R)$ is a

decreasing function of radius, $G(R)$ is positive and angular momentum is transported from small radii to large radii. This is essential if we want to have accretion: material at small radii gives its angular momentum to material at larger radii and moves inwards to a region where the specific angular momentum is smaller. The above result is clearly correct and also reproduces the intuitive behaviour of viscous circularly shearing motion. However, some difficulties arise when one tries to explain this behaviour in terms of kinetic theory, as often done, for example in many textbooks (Frank et al., 2002; Hartmann, 1998). This difficulty has been pointed out by Hayashi and Matsuda (2001) and solved by Clarke and Pringle (2004). In the kinetic theory approach, transport is determined by the collisions of fluid elements moving between different orbital radii due to random velocities. Thus, particles are emitted with random velocity at some radius with some specific angular momentum, move to a different radius where they collide and release their angular momentum, which in general is different from the specific angular momentum at the new location, thus leading to mixing and transport of angular momentum. The problem here is that naively calculating the resulting angular momentum flux due to this process (Hayashi and Matsuda, 2001) gives (as one might expect) the result that the flux is proportional to the negative gradient of the specific angular momentum, rather than the correct result (where the flux is proportional to the negative gradient of the angular velocity). This is perfectly analogous to the case of a linear shear flow, where the arguments above (also found in many textbooks of hydrodynamics) lead to the conclusion that, in this case, the linear momentum flux is proportional to the negative gradient of linear momentum.

If really the angular momentum flux was proportional to $-\nabla R^2 \Omega$ rather than to $-\nabla \Omega$, this would be disastrous for accretion discs. Indeed, if we consider the case of Keplerian discs, we see that while $\nabla \Omega$ is directed inwards (leading to an outward angular momentum flux), we have that $\nabla R^2 \Omega$ is directed outwards, leading to an inward flux of angular momentum, which would totally preclude accretion. Even worse, in the simple case of a spreading ring (described in more detail below), if really angular momentum were diffused down its gradient (which in this case is directed outwards), rather than spreading under the action of viscosity, the ring would tend to collapse in an infinitesimally thin annulus!

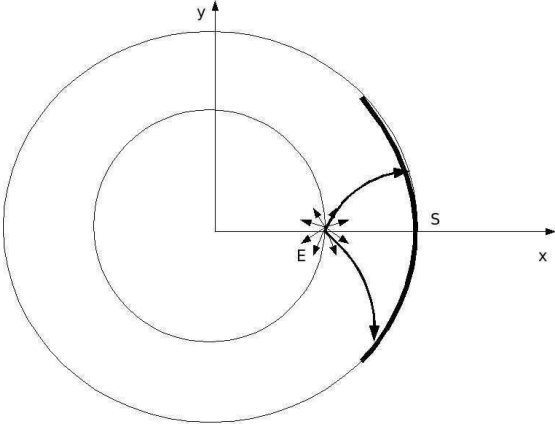


Fig. 3. Disc viscosity from kinetic theory. Sketch of the angular momentum flux from emission point E to reference surface S as seen in a reference frame corotating with E . Even if particles are emitted isotropically at E , due to Coriolis force, their path is not straight and they tend to intersect the reference surface S more normally if they are emitted in a prograde direction and more tangentially if they are emitted in a retrograde direction, thus enhancing the contribution of prograde particles to the flux at S .

The resolution of this difficulty was given by Clarke and Pringle (2004). The point is that even if the random distribution of particles is isotropic at the location where they are emitted, it is not isotropic at the position where they collide and release their angular momentum, and relatively more particles move on prograde orbits than retrograde ones. Thus, even if an annulus at a smaller radius has *on average* a smaller specific angular momentum than an annulus at a larger radius, it is preferentially those particles that happen to have an *excess* angular momentum that collide at a larger radius, releasing their angular momentum and so transporting it (correctly) from the inside out. The picture is even clearer if one considers the dynamics in a reference frame co-rotating with the emission location, E (see Fig. 3). In the (non-inertial) frame of E , particles are emitted isotropically. However, their path is not straight, due to the effect of Coriolis force. As seen in Figure 3, particles emitted in the prograde direction (that have an excess angular momentum with respect to E) tend to intersect a reference surface S more normally, while retrograde particles tend to intersect S on more tangential paths. Thus the contribution of prograde particles to the flux at S is larger than that of retrograde ones (see Matsuda and Hayashi 2004), thus removing the inconsistency.

Let us then summarise what we have learned so far. The radial component of the equation of motion generally takes the form of centrifugal balance, leading to

$$v_\phi = \sqrt{\frac{GM}{R}} \left[1 - \beta \left(\frac{c_s}{v_K} \right)^2 \right]^{1/2}, \quad (37)$$

thus indicating that rotation is Keplerian, with some correction terms due to pressure. The vertical equation of motion takes the form of hydrostatic balance, so that (in the non-self-gravitating case) the vertical density profile is Gaussian with thickness

$$\frac{H}{R} = \frac{c_s}{v_K}, \quad (38)$$

which shows that in order for the disc to be thin we require $c_s \ll v_K$. Finally, conservation of angular momentum and the continuity equation for a Keplerian disc lead to the following diffusive evolutionary equation for the disc surface density Σ

$$\frac{\partial \Sigma}{\partial t} = \frac{3}{R} \frac{\partial}{\partial R} \left[R^{1/2} \frac{\partial}{\partial R} \left(\nu \Sigma R^{1/2} \right) \right]. \quad (39)$$

4.6. Time-dependent solutions

Clearly, the equations derived above have a limited applicability if we do not specify what the viscosity is, and in particular whether it depends or not on other disc properties, such as surface density, temperature, radius, etc. As will be discussed below, in some cases, the relationship between viscosity and surface density might even change the diffusive character of equation (35).

Nevertheless, we can still gain some insight into disc dynamics by considering a couple of simple cases, which were initially discussed by von Weizsäcker (1948) and Lüst (1952).

4.6.1. The spreading ring

Consider, for example, the case in which ν is simply a constant, independent of radius and Σ , and the initial condition for the surface density is an infinitesimally thin ring of mass m , whose shape is a δ function centered at some radius R_0 :

$$\Sigma(R, t = 0) = \frac{m}{2\pi R_0} \delta(R - R_0) \quad (40)$$

The solution to equation (35) in this case was found by Lynden-Bell and Pringle (1974):

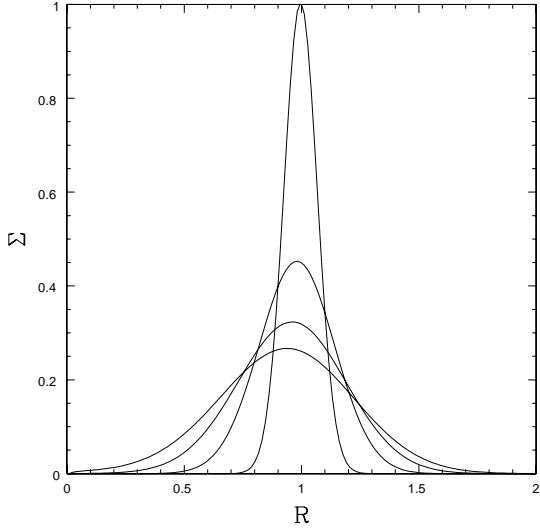


Fig. 4. Evolution of the surface density according to Eq. (35). In this case the viscosity ν is taken to be simply a constant and the initial surface density is a thin ring centered at $R = 1$. The various plots refer to $\tau = 0.01, 0.05, 0.1$ and 0.15 .

$$\Sigma(x, \tau) = \frac{m}{\pi R_0^2} \frac{x^{-1/4}}{\tau} e^{-(1+x^2)/\tau} I_{1/4} \left(\frac{2x}{\tau} \right), \quad (41)$$

where $I_{1/4}$ is a modified Bessel function of the first kind, $x = R/R_0$ and $\tau = 12\nu t/R_0^2$. Apart from the complicated form of the analytic solution above, a few important features can be already be seen. First of all, note that the solution only depends on time through the combination $\tau = 12\nu t/R_0^2$. This allows us to introduce a typical timescale for the viscous evolution of the disc, $t_\nu \sim R^2/\nu$. While this result has been obtained in the particular case of a spreading ring, its validity is absolutely general and is in fact implicit in the structure of equation (35) itself. The evolution of the surface density is shown in Fig. 4, where the different lines refer to different times $\tau = 0.01, 0.05, 0.1$ and 0.15 . This figure illustrates quite clearly why this example is called “the spreading ring”. We see here that what happens indeed is that under the action of viscous forces the disc, rather than merely accreting, spreads both inwards and outwards. This outward spreading is needed in order to conserve angular momentum. Viscosity acts on the fluid to redistribute angular momentum between different annuli, the total angular momentum being conserved. In this way, as the inner parts of the disc lose their angular momentum and accrete, the outer parts take up the excess angular momentum and move outward. A detailed analysis of the analytic solution (see Frank et al. 2002 and Pringle

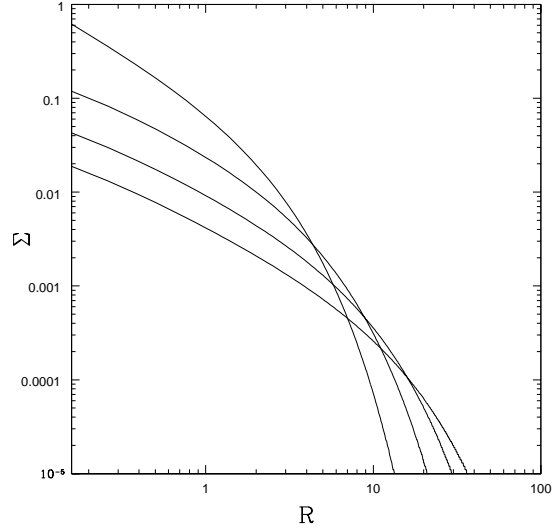


Fig. 5. Evolution of the surface density according to Eq. (35). In this case the viscosity $\nu \propto R$ and the solution is the self-similar solution (Lynden-Bell and Pringle, 1974). The solid lines show, from top to bottom, the self-similar solution at increasingly large times ($T = 1, 2, 4$ and 7 respectively).

1981) shows that the transition between inward and outward motion occurs at a radius of order $R_{\text{tr}} \sim t\nu/R_0 \sim R_0(t/t_\nu)$ and is therefore an increasing function of time. Therefore, at late times, only the outermost parts of the disc move outwards, and most of the mass is eventually accreted. For $t \rightarrow \infty$, all the mass in the ring is accreted and the angular momentum is transported to infinitely large radii by a negligibly small amount of mass.

4.7. Self-similar solutions

Another important class of solution (also discussed by Lynden-Bell and Pringle 1974) is found in cases where the viscosity has a simple power-law dependence on radius, $\nu \propto R^b$. In this case, it is possible to find a self-similar analytical solution. Let us consider the simple (but not too unrealistic, see also King 1998) case where $\nu \propto R$ and the initial density profile is such that accretion proceeds almost steadily out to a typical radius R_1 at which the density is exponentially truncated. A detailed derivation in this case can be found in Hartmann (1998). The surface density and the mass accretion rate \dot{M} as a function of time are given by:

$$\Sigma(R, t) = \frac{CT^{-3/2}}{3\pi\nu(R)} \exp\left(-\frac{R/R_1}{T}\right), \quad (42)$$

$$\dot{M}(R, t) = CT^{-3/2} \left[1 - \frac{2R/R_1}{T} \right] \exp\left(-\frac{R/R_1}{T}\right), \quad (43)$$

where $T = 1 + t/(R_1^2/3\nu(R_1))$ and C is just a normalization constant. Here again, we can see that the typical timescale over which the disc evolves is the viscous timescale $t_\nu \sim R^2/\nu$. This relation is particularly useful from an observational point of view. Indeed, if we were able to have reliable measurements of disc sizes (for example, from sub-mm observations) and an estimate of the viscous timescale (obtained, for example, by comparing the fraction of young stars with discs in young stellar clusters of different ages), we could obtain an estimate of the magnitude of “viscosity” in the disc. The evolution of the density in this case is plotted in Fig. 5. Also in this case, as for the spreading ring, the disc spreads significantly outwards, even if most of the mass is eventually accreted. The transition between inward and outward moving portion of the disc for the self-similar solutions occurs at a transition radius $R_{\text{tr}} \sim R_1(t/t_\nu(R_1))^{1/(2-b)}$ and therefore increases with time (for the particular case where $b = 1$ described above, we have that R_{tr} increases linearly with time). As the disc empties out, the accretion rate on to the star drops steadily.

A question naturally arises at this stage. If we observe a given sample of discs, should we expect their observed size to increase or to decrease with age? The answer to this question strongly depends on the sensitivity of our measurements. Let us consider the density plots shown in Fig. 5. If the sensitivity of our measurement is very high, so that we can detect surface densities as low as, say, 0.0001 in the scale of Fig. 5, then clearly as the age of the system increases, the observed size will increase as well. On the other hand, if the sensitivity is much lower and we can only detect surface densities larger than, say, 0.01 in the same scale, then the observed disc size will decrease with the age of the system.

4.8. Steady-state solution

Let us now look at the form of steady-state solutions of the disc equations for a Keplerian rotation curve. In a steady state, the continuity equation (7) becomes:

$$\dot{M} = -2\pi R v_R \Sigma, \quad (44)$$

where the constant \dot{M} is the mass accretion rate and the signs have been chosen in such a way that

when v_R is negative (i.e. directed inwards) the accretion rate is positive. Analogously, angular momentum conservation becomes:

$$\dot{M}\Omega R^2 - 3\pi\nu\Sigma\Omega R^2 = \dot{J} \quad (45)$$

where \dot{J} is the constant net flux of angular momentum, and is determined by two contributions: the first term on the left hand side, which indicates the angular momentum advected with the accretion process, and the second term, which indicates the outward flux produced by viscous torques.

\dot{J} is sometimes determined by using the so-called “no torque” assumption, according to which at the disc inner radius R_{in} the angular velocity profile flattens (due to the presence of a boundary layer where the disc connects to the central object) so that its gradient and therefore the viscous torque vanish, thus implying $\dot{J} = \dot{M}(\Omega R^2)_{\text{in}} = \dot{M}\sqrt{GM R_{\text{in}}}$. Inserting this in equation (45), we obtain:

$$3\pi\nu\Sigma = \dot{M} \left(1 - \sqrt{\frac{R_{\text{in}}}{R}} \right). \quad (46)$$

At large radii, $R \gg R_{\text{in}}$, the surface density and the viscosity satisfy the following simple relation:

$$\dot{M} = 3\pi\nu\Sigma, \quad (47)$$

that is, surface density and viscosity are inversely proportional (cf. the asymptotic behaviour of the self-similar solution, Fig. 5 and Eq. (42)).

5. Accretion disc energetics

5.1. Radial temperature profile

Up to now, we have emphasised the role of viscosity and of viscous torques in redistributing angular momentum through the disc, hence allowing accretion. On the other hand, as accretion takes place, a significant amount of gravitational potential energy has to be dissipated by viscous forces. Let us then calculate this quantity. Let’s consider the expression for the total torque exerted by an annulus on a neighbouring one at larger radius, Eq. (36). The net torque $G(R)$ exerted on an annulus of radial extent ΔR is given by:

$$G(R - \Delta R/2) - G(R + \Delta R/2) = -\frac{\partial G}{\partial R} \Delta R. \quad (48)$$

The power produced by this torque per unit radial interval is then:

$$-\frac{\partial G}{\partial R}\Omega = -\left(\frac{\partial}{\partial R}(G\Omega) - G\Omega'\right). \quad (49)$$

We then see that the annulus loses energy due to two different contributions: the first one is just the radial derivative of $G\Omega$ and is related to energy transport due to viscosity: when integrated over the disc surface it will vanish except for the energy transported out of the disc boundaries. The second term does represent energy dissipation due to viscosity and we can thus write the power dissipated per unit area by both sides of the disc as:

$$D(R) = \frac{-G\Omega'}{2\pi R} = \nu\Sigma(R\Omega')^2 = \frac{9}{4}\nu\Sigma\Omega^2, \quad (50)$$

where the last equality holds for Keplerian discs. We can also calculate the total power emitted by the disc in a steady state. If we assume that the disc extends to infinity, we have that the disc luminosity is:

$$\begin{aligned} L_{\text{disc}} &= \int_{R_{\text{in}}}^{\infty} 2\pi R D(R) dR \\ &= \int_{R_{\text{in}}}^{\infty} \frac{3GM\dot{M}}{2R^2} \left(1 - \sqrt{\frac{R_{\text{in}}}{R}}\right) dR = \frac{1}{2} \frac{GM\dot{M}}{R_{\text{in}}}, \end{aligned} \quad (51)$$

where we have also used equation (46). Note that the luminosity is only half of the potential energy lost by the accreting matter, the remaining half being needed to keep the disc in Keplerian rotation at R_{in} .

Another subtlety illustrates the role of energy transport due to viscous torques. Let us calculate the energy dissipated by an annulus of width ΔR , far from the inner boundary. This is given by:

$$2\pi R D(R) \Delta R = \frac{3GM\dot{M}}{2R^2} \Delta R. \quad (52)$$

Now, we know that $(GM\dot{M}/2R^2)\Delta R$ comes from the release of gravitational binding energy, but where does the rest come from? The extra energy is provided by the energy transported from the inner disc and indeed it can be shown that the energy transport term in equation (49) provides just the right amount of energy. Obviously (in order to satisfy global constraints) the situation is reversed at small radii (for $R < 9R_{\text{in}}/4$) where the energy dissipated is less than the energy released by accretion, the excess being transported outwards.

If the power from equation (50) is radiated away at R as thermal blackbody emission, we can then estimate the surface temperature of the disc from $D(R) = 2\sigma_{\text{SB}}T_s^4$, where σ_{SB} is Stefan-Boltzmann

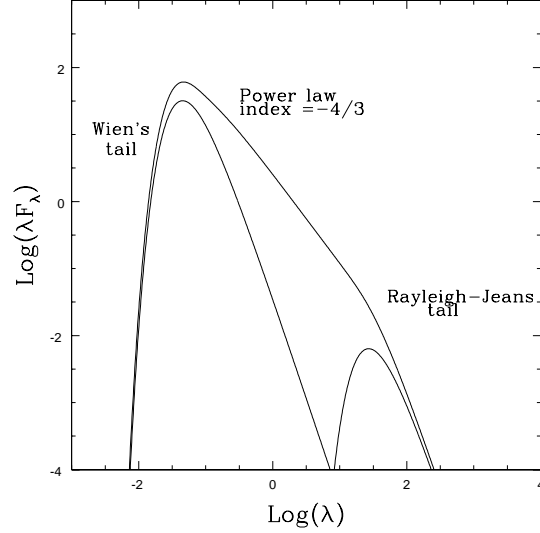


Fig. 6. Sketch of the SED of an actively accreting disc. The thick line is the full disc spectrum, while the two thin lines show two simple blackbody functions at T_{min} and T_{max} . The units in the axes are arbitrary. The SED looks like a stretched blackbody function. At long wavelengths $\lambda > hc/kT_{\text{out}}$, the SED approaches the Rayleigh-Jeans tail. At very short wavelengths $\lambda < hc/kT_{\text{in}}$, the SED has a sharp cut-off due to Wien's law, while at intermediate wavelengths the SED is a simple power law, with index depending on the temperature profile.

constant and where the factor 2 comes from the fact that the disc has two sides, so only half of $D(R)$ is radiated by each side. We thus get:

$$T_s^4(R) = \frac{3GM\dot{M}}{8\pi\sigma_{\text{SB}}R^3} \left(1 - \sqrt{\frac{R_{\text{in}}}{R}}\right), \quad (53)$$

Far from the inner boundary, the temperature profile of the disc has therefore the characteristic scaling $T_s \approx T_{\text{disc}}(R/R_{\text{in}})^{-3/4}$, where

$$T_{\text{disc}} = \left(\frac{3GM\dot{M}}{8\pi\sigma_{\text{SB}}R_{\text{in}}^3}\right)^{1/4}. \quad (54)$$

We thus see that the temperature profile of a viscously accreting disc in a steady state does not depend on viscosity. Actually, viscosity obviously implicitly enters in the determination of the temperature profile, by allowing the disc mass to be accreted at a given rate \dot{M} .

5.2. Disc spectral energy distribution

Now that we have obtained the temperature profile of the disc, we can calculate the expected spectral

energy distribution (SED). This is easily obtained under the assumption that the disc radiates as a blackbody, by integrating several blackbody spectra (with different temperature) over the disc surface. The flux F_λ emitted at wavelength λ is then:

$$\lambda F_\lambda = \frac{\cos i}{d^2} \int_{R_{\text{in}}}^{R_{\text{out}}} 2\pi R \lambda B_\lambda[T_s(R)] dR, \quad (55)$$

where d is the distance to the disc, i is the inclination and $B_\lambda(T)$ is the Planck function. The resulting SED is a superposition of several blackbody functions extending from the wavelength corresponding to the highest disc temperature T_{in} (which occurs in the inner disc) to the wavelength corresponding to the lowest temperature T_{out} (which occurs in the outer disc), and has the shape of a stretched blackbody function as shown in Fig. 6. At long wavelengths $\lambda > hc/kT_{\text{out}}$, the SED approaches the Rayleigh-Jeans tail. At very short wavelengths $\lambda < hc/kT_{\text{in}}$, the SED has a sharp cut-off due to Wien’s law, while at intermediate wavelengths the SED is a simple power law, with index depending on the temperature profile. It is possible to show (Adams et al., 1988) that if the temperature profile is a power-law with index $-q$, then the power-law index of the disc SED λF_λ at intermediate wavelengths is given by $n = 2/q - 4$. We then see that the temperature profile of an accreting disc $T_s \propto R^{-3/4}$ leads to an SED with $\lambda F_\lambda \propto \lambda^{-4/3}$.

The full SED of an accreting protostar is given by the spectrum of the star, that, to a first approximation, can be represented by a single blackbody spectrum at the temperature of the stellar photosphere, plus the spectrum of the accretion discs, whose temperature is much lower, so that the SED extends down to longer wavelengths, in the near and mid infrared. Indeed, the first evidence for the existence of discs around young stars came from observations of infrared excess with IRAS first (Beichman et al., 1986), and later with ISO.

While the simple expectation that disc SEDs span a relatively large range of wavelengths is generally confirmed by observations (especially in the infrared and sub-mm range), a detailed comparison of the model described above with observed disc SED has proven to be more problematic. Indeed, in most cases, observed SEDs show significant departures from the standard power-law with index $n = -4/3$. The cleanest example where the observed SED of a protostellar disc is well reproduced

by the “standard” disc SED as described above (at least over a sizeable wavelength range), is the case of FU Orionis objects (Kenyon et al., 1988; Kenyon and Hartmann, 1991). Such objects are outbursting objects (see also below) and their accretion rates can be very large, of the order of $10^{-5} - 10^{-4} M_\odot/\text{yr}$ (for a review, see Hartmann and Kenyon 1996).

For most circumstellar discs, such as those observed around T Tauri and Herbig Ae/Be stars, the infrared SED is much flatter than predicted from the active disc model above, indicating a much shallower radial temperature profile. In particular, most cases are consistent with a temperature profile of the form $T_s \propto R^{-1/2}$ (Beckwith et al., 1990). Indeed, the above description does not take into account an important heating term for the disc: irradiation from the central star. The effect of stellar irradiation on the disc temperature profile has been considered by Adams and Shu (1986) and Adams et al. (1988). Interestingly, it turns out that the temperature profile for a flat disc (that is, a disc with constant thickness H) dominated by irradiation is given by:

$$T_{\text{irr}} \approx T_\star \left(\frac{R}{R_\star} \right)^{-3/4}, \quad (56)$$

where T_\star and R_\star are the stellar temperature and radius, respectively. This can be simply understood as follows. The stellar flux at the surface of the star is $\approx \sigma_{\text{SB}} T_\star^4$. At a distance R from the star, the flux is decreased by a factor $(R/R_\star)^{-2}$. An additional factor $(R/R_\star)^{-1}$ comes from geometrical considerations. Since the disc is flat, it absorbs only a fraction $\sin \theta \approx \theta$ of the stellar flux, where $\theta \approx R_\star/R$ is the angle under which the star is seen from the disc. We thus see that, including irradiation on a flat disc still produces a steep temperature profile (in fact, the same kind of profile obtained for an accreting disc), which remains inconsistent with observations.

In fact, the above result is not entirely self-consistent. The point is that if the temperature is $\propto R^{-3/4}$, we then have that the sound speed $c_s \propto R^{-3/8}$ and the thickness $H = c_s/\Omega \propto R^{9/8}$. The disc thus “flares” in the outer regions, with the aspect ratio H/R increasing with radius. The outer parts of the disc will thus absorb a larger fraction of the stellar flux and the temperature profile will not be as steep as predicted above. Kenyon and Hartmann (1987) have considered self-consistent models of such flared disc, and found that in this way it is possible to broadly reconcile the models with the observations, and to reproduce the required profile

$T \propto R^{-1/2}$. Chiang and Goldreich (1997) have further elaborated on these models, and propose that the disc at a given radius can simply be represented by two zones: an upper, hot layer (much hotter than the temperature predicted by a simple blackbody model) that absorbs efficiently the stellar radiation and re-emits half of it, and a cooler layer below, which reprocesses the remaining half and re-emits thermally in the infrared. Recent models of disc SED (see, for example, Dullemond et al. 2001) are generally variations on this basic simple model. An up to date account of such modeling can be found in Dullemond et al. (2007).

Finally, it is important to stress that (apart from a few exceptions) in most cases discs around young stars are neither entirely “active” (that is, with SED dominated by accretion) nor “passive” (that is, with SED dominated by irradiation). In general both internal and external heating will provide some contribution, the relative importance of the two being determined by a comparison of accretion versus stellar luminosity. It is then interesting to see that (for a young solar type star) the two contributions are comparable for accretion rates of the order of $10^{-8} M_{\odot}/\text{yr}$ (Armitage, 2007), which falls roughly in the middle of the range of accretion rates observed for T Tauri stars.

6. Timescales

Before moving on to discuss several instabilities that might occur in accretion discs, it is useful to briefly consider what are the various timescales over which accretion discs form and evolve. We have already encountered a few important timescales. First of all, we have the dynamical timescale, which is simply related to the orbital period T . We have:

$$t_{\text{dyn}} = \Omega^{-1} = \frac{T}{2\pi}. \quad (57)$$

This is roughly the time needed to reach centrifugal equilibrium and, for a Keplerian disc, it scales with $R^{3/2}$ (in particular, $t_{\text{dyn}} = \sqrt{R^3/GM}$). This is also the typical growth time of some important instabilities, such as the magnetorotational and gravitational instability, discussed below. A second important timescale is the vertical timescale, needed to reach hydrostatic balance in the vertical direction. This is given by the sound crossing time across the disc thickness H :

$$t_z = \frac{H}{c_s} = \Omega^{-1} = t_{\text{dyn}}. \quad (58)$$

Interestingly, this timescale is equal to the dynamical one. A simple understanding of this can be obtained as follows. Consider a fluid element at the top surface of the disc. If this element moved on an exactly Keplerian orbit around the central star, after half a period it would be on the bottom surface (and similarly a fluid element at the bottom would move to the top after half a period). In order to prevent this, and to keep the ‘top’ to stay on top, the fluid element needs to receive an upward force, provided by pressure, that has to be effective on the short orbital (and therefore dynamical) timescale.

A third timescale is the thermal timescale t_{th} , which corresponds to the time needed by the disc to modify its thermal structure, and its temperature. In general, we will have a cooling timescale t_{cool} which is set by the specific cooling processes in the disc, and a heating timescale t_{heat} which (for active discs) is determined by energy release due to accretion. In thermal equilibrium, clearly these two timescales are equal. If we refer to the heating timescale, this is simply given by the ratio between the heat content at a given radius and the power produced by accretion (eq. (50)):

$$t_{\text{th}} = \frac{\Sigma c_s^2 / (\gamma(\gamma - 1))}{\nu \Sigma (R\Omega')^2} = \frac{4}{9\gamma(\gamma - 1)} \frac{1}{\alpha\Omega}, \quad (59)$$

where γ is the ratio of the specific heats and where we have also used the so-called α -prescription for viscosity (that will be described more in detail below in section 8), according to which $\nu = \alpha\Omega H^2$, where α is a dimensionless parameter smaller than unity. We thus see that $t_{\text{th}} \sim t_{\text{dyn}}/\alpha \gg t_{\text{dyn}}$.

Finally, we have the viscous timescale, which sets the scale for the evolution of the surface density. From the analysis of time-dependent models above, we have seen that this timescale is given by:

$$t_{\nu} = \frac{R^2}{\nu} = \left(\frac{H}{R}\right)^{-2} \frac{1}{\alpha\Omega} \gg t_{\text{th}}, \quad (60)$$

where again we have used the α -prescription. We thus see that the various timescales are ordered in the following way:

$$t_{\nu} \gg t_{\text{th}} \gg t_z \sim t_{\text{dyn}}, \quad (61)$$

which then shows that the centrifugal balance in the radial direction and hydrostatic balance in the vertical direction are very rapidly achieved, while the disc temperature generally evolves on a longer timescale, and finally, on an even longer timescale,

one can see some evolution in the surface density profile.

Finally, note that all of the above timescales are a function of radius. In particular, if α and H/R are constant (which is not generally true), then they all scale in the same way, and for a Keplerian disc, they increase with radius as $R^{3/2}$. Thus the evolution of the inner disc is generally much more rapid than the evolution of the outer disc.

7. Limit cycle instability and FU Orionis outbursts

Accretion discs can be subject to a large number of instabilities: from the standard thermal instability (which occurs when the net heating rate at a given pressure is an increasing function of temperature), to the very important instabilities which occur when some physical effects ignored so far (such as magnetic fields or the disc self-gravity) are included. Given the importance of the latter instabilities in providing some likely mechanism to transport angular momentum, we will discuss them in more detail below. In this section we will rather focus on another kind of instability (the so-called “thermal-viscous”, or “limit cycle” instability), which is particularly relevant to some circumstellar discs. This instability was first discussed in the context of accretion discs in evolved galactic binaries, and in particular it is very successful in explaining the so called “dwarf novae” outbursts (Faulkner et al., 1983; Papaloizou et al., 1983; Lin et al., 1985). In the context of discs around young stars, it has been very often considered as the likely outburst mechanism for FU Orionis outbursts (Hartmann and Kenyon, 1996), even if its application to this class of system is somewhat less successful.

Let us reconsider Equation (35) above. As mentioned above, this is a simple diffusion equation for the surface density Σ . However, this is strictly true only in the case in which the viscosity ν is not dependent on Σ . Of course, in general ν can be a function of radius, temperature and even density. In the latter case, the equation becomes a non-linear equation for Σ for which the solution can be much more complicated than the simple cases described above. Some interesting behaviour can be predicted also in this more general case (Frank et al., 2002). In fact, when ν is a function of Σ , eq. (35) can be re-written in terms of the variable $\mu \equiv \mu(\Sigma) = \nu\Sigma$, which is proportional to the net flux of matter across a disc

annulus. We have then:

$$\frac{\partial\mu}{\partial t} = \frac{\partial\mu}{\partial\Sigma} \frac{3}{R} \frac{\partial}{\partial R} \left[R^{1/2} \frac{\partial}{\partial R} (\mu R^{1/2}) \right]. \quad (62)$$

Now, when the coefficient $\partial\mu/\partial\Sigma$ is positive, the evolution equation for μ is still a diffusion equation with no particular problems. However, when $\partial\mu/\partial\Sigma < 0$ the character of the equation changes and we have an instability. A simple interpretation of the nature of this instability can be given if we consider that μ is nothing else than the net mass flux out of a given disc annulus. Therefore, if at a given radius, following a decrease in Σ , the flux μ increases, this will cause a further reduction in Σ and therefore it will trigger a runaway behaviour at that radius. We now need to ask whether it can ever happen that $\partial\mu/\partial\Sigma < 0$. Since ν is in general a function of disc density and temperature, the detailed relation between μ and Σ will depend on the detailed thermal structure of the disc. Specific models of this relation for discs around young stars have been provided by Bell and Lin (1994), based on detailed opacity laws appropriate for circumstellar discs. The relationship between μ and Σ obtained by Bell and Lin (1994) can be seen in Fig. 7. The upper panel shows the opacity coefficient used by Bell and Lin (1994) as a function of temperature and for different disc densities (indicated by different solid lines), while the lower panel shows the $\mu - \Sigma$ relation in thermal equilibrium derived in this case, where the different lines refer to different disc radii. It can be seen that they have a typical *S*-shape, and that for mass fluxes of the order of $10^{-6} M_{\odot}/\text{yr}$ (almost independent on radius) we have indeed an unstable configuration with $\partial\mu/\partial\Sigma < 0$. The kinks in the $\mu - \Sigma$ curves correspond to temperatures between 10^3K and 10^4K , where the opacity shows a sudden steep rise due to partial ionization of hydrogen.

The evolution of the system can be qualitatively described as follows. Let us consider a given radius in the disc (say, the one corresponding to the rightmost curve in the lower panel of Fig. 7). Let us assume that initially the disc density is low (say, less than $10^5\text{g}/\text{cm}^2$, on the lower branch of the *S*-curve) and that the disc is fed at a rate of the order of $10^{-6} M_{\odot}/\text{yr}$. Since the equilibrium mass flux corresponding to the disc density is much smaller than the flux at which the disc is fed, the density will rise, moving up the curve, until the density reaches the maximum value at which the annulus is stable (corresponding to the “kink” in the *S*-curve). At this point the thermal-viscous instability is trig-

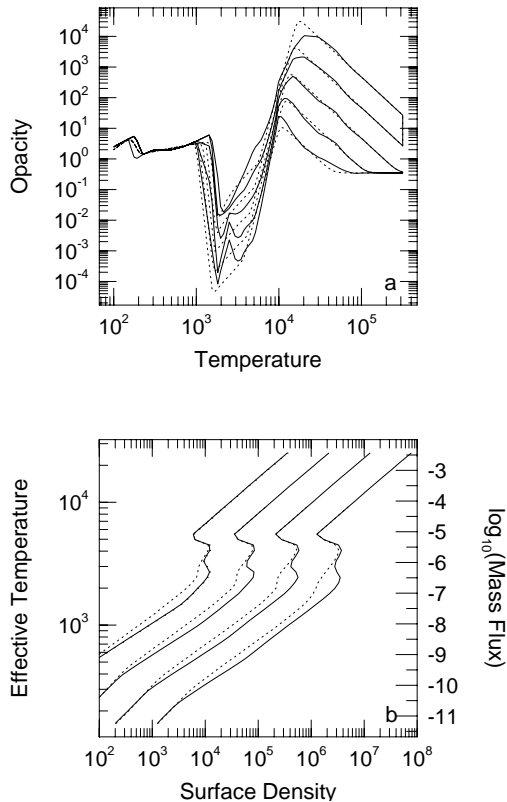


Fig. 7. Upper panel: opacity coefficient as a function of temperature (the different curves refer to different densities). Lower panel: the resulting relation between mass flux μ and surface density (the different curves refer to different radii in the disc). Figure from Bell and Lin (1994). The units are such that the temperature is in K, the mass flux is in M_{\odot}/yr , the surface density is in g/cm^2 and the opacity in cm^2/g .

gered and the temperature and the local mass flux will jump up to the upper branch of the S -curve, to the stable value at that density (which in this example corresponds to a mass flux of the order of $10^{-4}M_{\odot}/\text{yr}$). Now, the mass flux in the upper branch is much larger than the rate at which the disc is fed, so that the density will slowly decrease down to the minimum stable density in the upper branch of the S -curve. This then causes another jump in the mass flux down to a stable solution in the lower branch and the whole process will repeat again, leading to a limit cycle in which the mass flux at this radius oscillates between a high value of the order of $10^{-4}M_{\odot}/\text{yr}$, corresponding to an outburst phase and a low value of the order of $10^{-7}M_{\odot}/\text{yr}$, corresponding to a quiescent phase. On average, over long periods of time the mass accretion rate will be of the order of the feeding rate $\approx 10^{-6}M_{\odot}/\text{yr}$.

The above arguments apply to the behaviour of a

single annulus of the disc, assumed to be independent on the neighbouring ones. Of course, in general we should solve the full equation and consider the interaction of the various annuli. This analysis (Lin et al., 1985) reveals a number of important features. Once the instability is triggered at some radius, at which the temperature is high enough to cause hydrogen ionization, two instability (ionization) fronts develop: a fast one, moving inwards (in an “avalanche” fashion, to use the terminology of Lin et al. 1985) and a slow one moving outwards (in a “snowplough” fashion). When the ionization front reaches the innermost parts of the disc, the instability will result in a large increase of the optical and infrared flux emitted by the disc and the rising timescale for the luminosity corresponds to the speed at which the instability front reaches the inner disc. The outward moving front moves out to a limiting radius, corresponding to the lowest surface density that can be stable in the high state. The disc is then characterized by an inner outbursting region and an outer region which remains in the low state. After a time of the order of the viscous timescale at the outer edge of the outbursting region, the disc locally drops down to the low state and the instability retreats from the outside in, leaving an inner disc which has been essentially emptied out by the outburst and is ready to be slowly filled up again, eventually leading to a new outburst. This recurrent behaviour is very often observed in evolved binary systems such as dwarf novae and an example of a model reproducing this behaviour in this context can be seen in Fig. 8, kindly provided by Patrick Deegan and Graham Wynn, which shows the evolution of the accretion rate of a typical dwarf nova outburst.

7.1. *FU Orionis* outbursts

How does the behaviour described above compare to observations of discs around young stars? As mentioned above, the limit cycle instability model has been often used to describe *FU Orionis* outbursts (for a detailed review, see Hartmann and Kenyon 1996). *FU Orionis* objects are a small class of protostellar systems undergoing large outbursts, during which their luminosity increases by as much as three orders of magnitude. Unfortunately only a very small number of such systems have been observed and in only three cases (the prototypical *FU Ori*, *V1057 Cyg* and *V1515 Cyg*) do we have a detailed knowledge of the lightcurve over a long period

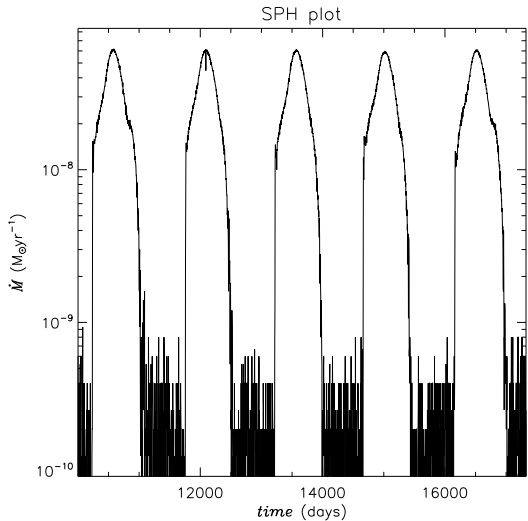


Fig. 8. Recurrent outbursts due to limit cycle instability in binary systems. Here the mass accretion rate as a function of time is displayed. Courtesy of Patrick Deegan and Graham Wynn.

of time, enabling us to gain some insight on their evolution and therefore on the dynamics of the outburst. Fig. 9 shows the light curve of these three objects (from Clarke et al. 2005). A first thing to notice is that the lightcurves of these three prototypical objects differ substantially between each other: while V1057 Cyg and FU Ori show a sharp rise to the high state (with a rise timescale of the order of 1 year), V1515 Cyg shows a much slower rise (~ 10 years). Once in the high state, while V1515 Cyg and FU Ori showed a very slow decline in luminosity, V1057 Cyg has dropped down almost to the original state within 10 years. Additionally, V1057 Cyg and V1515 Cyg have shown some rapid variability in the high state, while FU Ori has not. Reconciling such diverse behaviour within a single simple model is not easy but the limit cycle instability scenario, as will be discussed below, has managed to some extent in the challenge. On the other hand, several uncertainties remain, and the evidence in favour of it is much weaker than in the case of dwarf novae. A big disadvantage with respect to the case of dwarf novae is that the typical timescale of the outburst for FU Orionis is much larger than for dwarf novae and so it is not possible to observe repeated outbursts. On the other hand, the fraction of observed FU Orionis objects is consistent with each star undergoing a minimum of ~ 4 outburst throughout their life (Hartmann, 1998), which implies a duty cycle of at

least 10^4 years.

Hartmann and Kenyon (1985) and Kenyon et al. (1988) have shown how the spectral energy distribution of FU Orionis objects is to first approximation consistent with the one expected from a standard steady state accretion disc (as sketched, for example, in Fig. 6). Indeed, this is essentially the only clear case where a disc around a young star displays the typical emission feature of an active disc. While alternative interpretations have been suggested (e.g., Herbig et al. 2003), there is now a general agreement that the emission in FU Orionis systems is due to an actively accreting disc. Detailed modeling (Kenyon et al., 1988) shows that the typical accretion rates are of the order of $10^{-4} M_{\odot}/\text{yr}$.

The agreement however only holds at relatively short wavelengths, in the optical and near infrared, while in the mid infrared a substantial excess emission with respect to the expected disc spectrum is observed. Disc flaring, resulting in a shallower temperature profile (as for passive discs, see above) does not help much, since in this case it is the emission from the inner disc (rather than the star) to heat up the outer disc and the degree of flaring needed to reproduce the SED is too large (Kenyon and Hartmann, 1991). The mid infrared emission is therefore usually attributed to a dusty envelope (Kenyon and Hartmann, 1991). Alternatively, if the outer parts of the disc (beyond ~ 10 AU) are self-gravitating (see also below), the outer disc temperature might also be higher than for a standard disc, and indeed detailed self-gravitating disc models can reproduce the SED also in the mid infrared (Lodato and Bertin, 2003).

Recent infrared interferometry has played a major role in our understanding of FU Orionis objects. Malbet et al. (1998) and Malbet et al. (2005) have obtained infrared (H and K) interferometric data of FU Ori itself, showing that the infrared emission comes from an extended source (a few AU), consistent with the temperature profile expected for a disc, and providing possibly the definitive piece of evidence in favour of an active disc interpretation. Millan-Gabet et al. (2006) have observed (again, in the K band) other FU Orionis sources and found that in general the objects appear more resolved than would be expected from a simple disc model, implying emission from relatively hotter gas at larger distances. This is not inconsistent with the evidence coming from SED modeling which also implies a shallower temperature profile. However, simply changing the temperature power-law index

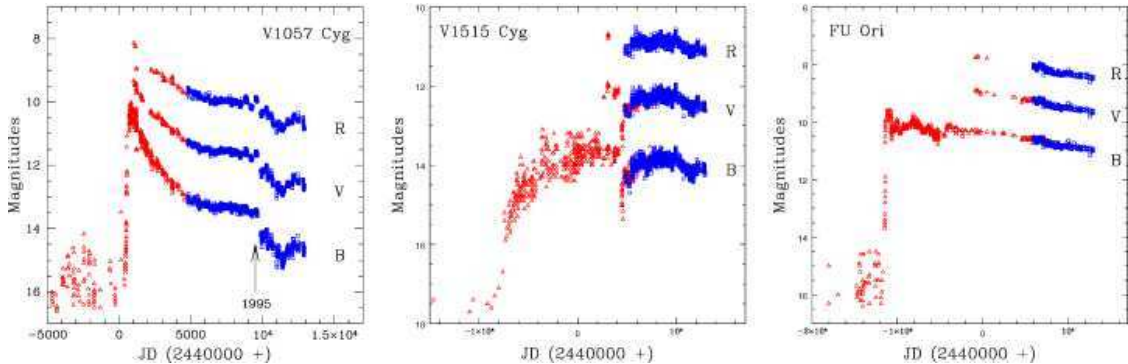


Fig. 9. B, V and R lightcurves of FU Ori, V1057 Cyg and V1515 Cyg. From Clarke et al. (2005).

does not reconcile the models with observations and Millan-Gabet et al. (2006) attribute the excess emission to a dusty envelope. No attempt to fit the data with a non power-law temperature profile (as used, for example, by Lodato and Bertin 2003 for their SED modeling) has been done. Additionally, it is worth noting that FU Orionis objects are not in a steady state, so the use of steady state models may not be appropriate. Indeed, Clarke et al. (2005) have shown that time-dependent models provide a better match to the colour evolution of V1057 Cyg and of V1515 Cyg at the beginning of the outburst.

So, despite all the caveats above, there is significant evidence that FU Orionis objects are indeed actively accreting accretion discs. What about the outburst mechanism? The limit cycle instability described above has the attractive features that (a) it does provide outbursts with the correct luminosity amplitude and that (b) it can in principle account for recurrent outbursts as required by number statistics. More subtly, it is also able to account for the different rise timescales in the three best studied objects. As discussed above, the rise timescale corresponds to the time taken for the instability front to travel through the inner disc. Now, if the instability is first triggered in the innermost parts of the disc, it will be the slowly moving outward front that determines the rise timescale, which will be relatively slow (as for V1515 Cyg), while if for some reason the instability is triggered at some distance from the star (of the order of a few tens R_{\odot}), it will be the fast (‘avalanche’) inward moving front that determines a fast rise time (as for FU Ori and V1057 Cyg). Detailed models of triggered and untriggered outbursts have been shown to reproduce roughly this behaviour (Clarke et al., 1989, 1990; Bell et al., 1995), by imposing some *ad hoc* triggering event. Clarke and Syer (1996) have suggested the interest-

ing proposal that the triggering agent might be a ‘hot Jupiter’ embedded in the pre-outburst disc (the presence of which might also have an observable effect in the optical and near infrared absorption line profiles, Clarke and Armitage 2003; Herbig et al. 2003). Detailed models using a planet to trigger the outburst have been discussed by Lodato and Clarke (2004) and Clarke et al. (2005), who also provide a detailed comparison with observations.

The real Achilles’ heel for such limit cycle instability models for FU Orionis objects is its inability to reproduce the outburst duration and its duty cycle. As discussed above, the outburst duration is set by the viscous timescale in outburst at the outer disc radius at which the instability can propagate. A simple estimate of this radius can be given by calculating, for a given input \dot{M} , the radius at which the temperature is high enough for partial hydrogen ionization. For an input rate of $10^{-6} M_{\odot}/\text{yr}$ (needed to reproduce the outburst amplitude), this radius turns out to be $\sim 20 R_{\odot}$ (Hartmann, 1998). Now, unless the disc viscosity is very low (so that the parameter α , commonly used to measure disc viscosity, is $\approx 10^{-3}$), the viscous timescale at this radius is much shorter than the tens of years observed as outburst duration. Actually, the instability front can overshoot to significantly larger radii (especially in the case of triggered outbursts) and more detailed calculations (Lodato and Clarke, 2004) give an outer propagation radius $\sim 40 R_{\odot}$, which however, only slightly improves the situation. Even worse, the duty cycle of the outburst is determined by viscosity in the quiescent phase, and even reducing α to 10^{-4} still results in a duty cycle of the order of a few 10^3 years, which is only marginally consistent with the expectations of at least 10^4 years.

Alternative outburst mechanisms have been proposed. For example, Vorobyov and Basu (2005,

2006) attribute them to the variability associated with a gravitational instability in a massive disc (this will be discussed in more detail below in Section 8.7). Armitage et al. (2001) invoke a combination of gravitational instability and the magneto-rotational instability in layered discs (see Section 8.6). However, a detailed calculation of the resulting rise timescale and outburst duration in these cases has not yet been performed. If indeed the origin of the outburst lies in some form of gravitational instability, then it is interesting to note that this would also naturally produce a non power law temperature profile that would fit the mid infrared SED and possibly the resolved interferometric observations (Lodato and Bertin, 2003).

Yet another possibility is an enhancement in accretion rate as a consequence of binary interaction with a companion star (Bonnell and Bastien, 1992), a hypothesis reinforced by the recent observations of a companion to FU Orionis itself (Wang et al., 2004). However, the distance of the companion in this case (≈ 200 AU) is so large that its dynamical timescale far exceeds all the observed outburst timescales, so it is hard to see how such a distant companion can cause a sudden rise in luminosity in a time as short as one year.

In summary, despite the limitations and the difficulties of the limit cycle instability model for FU Orionis, at present there has not been any attempt to provide a detailed alternative model, able to reproduce the various timescales involved and to fit the observational data.

8. Disc “viscosity”: the α -prescription and beyond

Up to now, we have avoided a discussion about what physical processes are responsible for disc “viscosity” and its expected magnitude. In this way, we have emphasised what can be done without a detailed knowledge of the viscosity (for example, the SED of an actively accreting disc) and especially what cannot be done (viscosity is essential in setting the relevant timescale of evolution of discs, so evolutionary models, as we have seen for FU Orionis, do depend strongly on the nature of viscosity).

The issue of viscosity has historically been a key issue in accretion disc physics. As it was early realized, and as we will show here below, standard kinetic viscosity due to collisions between gas molecules is far too low to account for the transport of angu-

lar momentum needed in observed accretion discs. For decades, modelers have relied on a very simple and successful parameterization of viscosity in terms of an unknown dimensionless parameter, called α (Shakura and Sunyaev, 1973). This α -prescription has been widely used, and we have also referred to it above, when we needed to give an order of magnitude estimate of viscosity. From the beginning of the '90s, increased computer power made it possible to run complex hydrodynamical and magneto-hydrodynamical simulations of discs. These made possible a careful examination of the fluid instabilities the disc might be subject to, and finally gave an idea of the long-sought nature of angular momentum transport in discs. At present, this issue is probably the key outstanding research topic in the theoretical modeling of accretion discs.

It is commonly thought that accretion discs are turbulent and that transport arises from the fluctuations associated with turbulence. Turbulence is supposed to arise as a consequence of the development of MHD instabilities, and in particular of the so-called magneto-rotational instability (MRI, Balbus and Hawley 1991), that will be briefly summarized below and discussed in more detail in the Chapter by Ferreira. While there is still some debate on whether pure hydrodynamic discs can be non-linearly turbulent (Richard and Zahn, 1999; Mukhopadhyay et al., 2005; Lesur and Longaretti, 2005; Ji et al., 2006), it is highly likely that some other physical process rather than pure hydrodynamics has to be at work, in order for significant transport to take place. If discs are relatively massive (as can happen in the early stages of star formation) gravitational instabilities might provide the required mechanism. In recent years there has been a substantial effort in describing the evolution of gravitationally unstable discs, and I will summarize the recent progress on this issue in section 8.7 below.

8.1. *The magnitude of collisional viscosity*

Before embarking on a discussion on ‘anomalous’ viscosity and what might cause it, it is instructive to see why ‘standard’ viscosity, which we are familiar with, does not provide enough stress to power disc accretion. In order to see this, let us consider the viscous timescale introduced above, $t_\nu = R^2/\nu$. It is convenient to express this quantity in units of the dynamical timescale $t_{\text{dyn}} = \Omega^{-1}$:

$$\frac{t_\nu}{t_{\text{dyn}}} = \frac{R^2 \Omega}{\nu}. \quad (63)$$

Note that the ratio above is nothing other than the Reynolds number Re of the flow. Standard, collisional viscosity can be expressed as the product of the typical random velocity of molecules (that will be of order of the sound speed c_s) and the collisional mean free path $\lambda = 1/(n\sigma_{\text{coll}})$, where n is the number density of the gas and σ_{coll} is the collisional cross-section. We then have:

$$\lambda = \frac{1}{n\sigma_{\text{coll}}} = \frac{\mu m_p}{\rho \sigma_{\text{coll}}} = \left(\frac{\mu m_p}{\Sigma \sigma_{\text{coll}}} \right) H, \quad (64)$$

where $m_p \approx 10^{-24}$ cm is the proton mass, μ is the average molecular weight (we can take it to be ≈ 2 , for simplicity) and where ρ and Σ are the usual volume and surface density of the disc, respectively. Now, substituting $\nu = \lambda c_s$ in equation (63), we get:

$$\frac{t_\nu}{t_{\text{dyn}}} = \left(\frac{\Sigma \sigma_{\text{coll}}}{\mu m_p} \right) \left(\frac{H}{R} \right)^{-2}. \quad (65)$$

To give some ideas of the numbers involved, let us assume that the collisional cross section is simply of the order of the size of an hydrogen molecule $\sigma_{\text{coll}} \approx 10^{-16}$ cm². In order to give a rough estimate of the disc surface density let us assume that the disc mass is $\approx 0.005 M_\odot$ and that the disc size is ≈ 50 AU, which gives us $\Sigma \approx 0.005 M_\odot / (50 \text{ AU})^2 \approx 10 \text{ g/cm}^2$. Inserting this numbers in Eq. (65), and also assuming that $H/R \approx 0.1$, we get $t_\nu/t_{\text{dyn}} \approx 10^{11}$. Since the dynamical timescale is of the order of a few years, the above estimates would lead to the conclusion that in order to accrete a disc of mass $0.005 M_\odot$ from a distance of 50 AU, it would take much longer than the Hubble time! Clearly, the magnitude of viscosity must be much larger than the simple collisional one estimated above.

8.2. Turbulent transport

As remarked above, the ratio of the viscous timescale to the dynamical one is also equal to the Reynolds number of the flow. The fact that collisional viscosity gives such a large estimate of this ratio also implies that the Reynolds number of the accretion flow is correspondingly large. Now, it is well known that for high Reynolds numbers a flow is subject to the development of turbulence and we should therefore expect the flow in an accretion disc to be highly turbulent. In these conditions, viscosity can be much higher because in this case angular

momentum is exchanged not through collisions of individual gas molecules, but by the mixing of fluid elements moving around in the disc due to turbulence. The typical length-scale of such motion can be several orders of magnitude larger than the collisional mean free path and consequently transport becomes much more effective.

It is instructive to rewrite the fundamental equations of *non-viscous* hydrodynamics, separating the mean flow (let us call \mathbf{v} the mean velocity) from the fluctuating quantities (as done, for example, in Balbus and Hawley 1998). It is then possible to show that the angular momentum equation can be rewritten as:

$$\frac{\partial}{\partial t} (\Sigma R v_\phi) + \frac{1}{R} \frac{\partial}{\partial R} (R v_R \Sigma R v_\phi) = - \sum_i \frac{1}{R} \frac{\partial}{\partial R} \left(R^2 \Sigma \langle u_R^{(i)} u_\phi^{(i)} \rangle \right). \quad (66)$$

In Eq. (66) the angle brackets indicate a vertical and azimuthal average and the summation operates over the various fluctuating fields that contribute to the stress. In the simplest case of a purely hydrodynamic flow, the only relevant field is the velocity fluctuation field, and this contribution to the stress tensor (called the ‘‘Reynolds’’ stress) is:

$$T_{R\phi}^{\text{Re}} = -\Sigma \langle u_R^{\text{Re}} u_\phi^{\text{Re}} \rangle, \quad (67)$$

where \mathbf{u}^{Re} is simply the velocity fluctuation. In the case of a magnetized disc, the magnetic field \mathbf{B} provides another source of transport, leading to the so-called ‘‘Maxwell’’ stress:

$$T_{R\phi}^{\text{M}} = \Sigma \langle u_{A,R} u_{A,\phi} \rangle, \quad (68)$$

where $\mathbf{u}_A = \mathbf{B}/\sqrt{4\pi\rho}$ is the Alfvén velocity. Finally, if the disc is massive enough that its self-gravity is non-negligible, the perturbed gravitational field \mathbf{g} provides yet another source of transport, in the form:

$$T_{R\phi}^{\text{g}} = -\Sigma \langle u_R^{\text{g}} u_\phi^{\text{g}} \rangle, \quad (69)$$

where $\mathbf{u}^{\text{g}} = \mathbf{g}/\sqrt{4\pi G\rho}$ (Lynden-Bell and Kalnajs, 1972). Equation (66) shows that in the presence of a non-zero correlation between the radial and azimuthal components of any of the fluctuating fields described above, angular momentum can be removed from the mean flow. Indeed, comparing Eq. (66) to Eq. (31), it is readily seen that such correlations play exactly the same role as a viscous stress tensor as concerns angular momentum conservation.

8.3. Turbulent ‘viscosity’?

We have seen above that the stress provided by turbulent fluctuations plays exactly the same role as a viscous stress from Navier-Stokes equations. Is this enough to let us speak about a ‘turbulent viscosity’? Actually, before being able to do so, we should answer two important questions.

First of all, viscosity is a *dissipative* process which of course leads to energy dissipation (and indeed it is due to such dissipation that actively accreting discs are luminous). In the fluctuations dynamics described in the previous section, energy is being taken from the mean flow and given to the fluctuations, without really being dissipated. So, before really speaking about viscosity, we have to (a) make sure that for a given angular momentum flux the amount of energy transferred to the fluctuations is the same as would be dissipated in a viscous process (Eq. (50)) and (b) we have to address the issue of whether fluctuations are readily dissipated locally or instead whether they are able to travel significantly before being dissipated. The issue has not yet been settled completely. Balbus and Papaloizou (1999) have shown that while for Reynolds and Maxwell stresses the answer to question (a) above is positive, in the case of gravitational stresses some other ‘anomalous’ energy fluxes come into play. On the other hand, Gammie (2001) argues that such ‘anomalous’ fluxes are negligible, at least under some conditions (see Section 8.7 below for further details). The answer to question (b) above is even more subtle and there is no simple and general answer to it. Clearly, only large scale numerical simulations can give an answer to this question. In this respect, it is somewhat reassuring that most simulations performed to date (whether for magnetized or self-gravitating discs) do not find significant degree of non-local transport, thus suggesting that ‘turbulent’ transport does behave to first approximation as an ‘anomalous viscosity’.

A second subtlety is related to the fact that the viscous stress tensor is proportional to the rate of strain ($R\Omega'$), while Eqs. (67)-(69) do not immediately show this relationship. Indeed, it has been argued (Pessah et al., 2006) that (at least for magnetic stresses) this is not the case. This, however, would only have a significant effect in cases where the rotation law departs significantly from a Keplerian profile (or, more exactly, when $|\Omega'|$ is significantly different than Ω/R), which might occur in the presence

of large pressure gradients, for example in a boundary layer, close to the star.

8.4. The α -prescription

To summarize the discussion above, while the debate is still not settled, there is as yet no conclusive evidence that for most applications (for example, for calculating the blackbody spectrum of an active disc) it would be incorrect to take the simple assumption that transport is due to some kind of ‘anomalous’ viscosity, the magnitude of which is unknown.

How can we then estimate the magnitude of such viscosity in a simple way, based on fundamental physical arguments? Such an estimate has been provided in a seminal paper by Shakura and Sunyaev (1973). The argument is very simple and draws from the fact that the stress tensor has the physical dimension of a pressure, that is a density times the square of a velocity (as can be easily seen from Equations (67) to (69), keeping in mind that these equations refer to a vertically integrated stress). The simplest assumption is then to take the stress tensor to be just proportional to the vertically integrated pressure Σc_s^2 :

$$T_{R\phi} = \frac{d \ln \Omega}{d \ln R} \alpha \Sigma c_s^2, \quad (70)$$

where $d \ln \Omega / d \ln R$ ($\sim -3/2$ for a quasi Keplerian disc) is just a number (to remind us that the viscous stress is proportional to the rate of strain), and where α is the proportionality factor between the stress tensor and the pressure.

Another way of expressing the α -prescription is by considering the kinematical viscosity ν . Indeed, Eq. (70) is equivalent to:

$$\nu = \alpha c_s H. \quad (71)$$

This form of the α -prescription offers a simple way to put some constraints on α . The magnitude of turbulent viscosity is given roughly by $\nu \sim \hat{v} l$, where l is the typical size of the largest eddies in the turbulent pattern and where \hat{v} is the typical turbulent velocity. Now, it is unlikely that the turbulence will be highly supersonic, since otherwise it would easily dissipate through shocks and we thus have $\hat{v} \lesssim c_s$. An upper limit to the size of the largest eddies l is obviously given by the disc thickness H (if we consider an isotropic viscosity). These two upper limits, taken together, clearly imply that $\alpha < 1$.

Now, it is important to point out what the α -prescription is *not*. It is *not* a theory of viscosity in accretion discs. It is just a simple parameterization based on dimensional analysis. By introducing the α -prescription, we have not gained any insight in what is the disc viscosity. Without it, we do not know what the kinematical viscosity ν is, while by using it we are left without knowing what α is. We have simply moved our unknowns from viscosity to α . A way to look at the α -prescription is that it is just a measure of the disc internal stresses in units of the local pressure. It is in this sense that it is mostly referred to recently, and the numerical simulations results are often discussed in terms of the ‘equivalent α ’ produced by the turbulence. Another important thing to stress is that while α is often taken to be a constant, it obviously does not need to be so, and indeed in general it can be a function of radius, density, temperature, ionization level, etc...

As to the magnitude of α , the arguments above enable us to put an upper limit to it $\alpha \lesssim 1$, but this is of course a very loose constraint. A way to proceed is to calibrate α based on the few cases where some observed evolutionary behaviour can be compared to theoretical models. By far, the best constraints on α come from observations of dwarf novae outbursts (Lasota, 2001) where, as discussed above, the limit cycle instability provides a good theoretical fit to the observations and the various timescales of the outburst are indeed strongly dependent on α . This kind of analysis leads to value of $\alpha \approx 0.1$. Another way of estimating α comes from comparing the similarity solutions described in Section 4.7 with observations of a statistical sample of discs at different ages, assuming that we know the initial size distribution. This has been done by Hartmann et al. (1998) (and more recently by Andrews and Williams 2007) and the observations seem to require a value of $\alpha \approx 0.01$. While this is lower than that inferred for dwarf novae outbursts, these values might not be inconsistent with each other, especially if ‘viscosity’ is driven by MHD instabilities, which are expected to be more effective in the hot and highly ionized environment of dwarf novae than in a cold disc around a young star. On the other hand, as has been noted above, modeling FU Orionis outbursts in terms of a limit cycle instability requires much lower values of $\alpha \approx 10^{-4} - 10^{-3}$. Now, while clearly this represents a big stumbling block for the application of the limit cycle instability to FU Orionis object, on the other hand it is important to stress that since such objects are essentially the only protostellar discs whose lu-

minosity is clearly dominated by accretion, it would be highly valuable to develop consistent accretion models for them, as this would give the best insight on the magnitude of viscosity in this context.

8.5. Hydrodynamic instabilities?

Now, having seen what the magnitude of viscosity is expected to be based on the observational evidences for a number of different cases, we should turn to theory and ask what can be provided by detailed modeling of turbulent discs. First of all, however, we should ask why should a disc be turbulent at all. We have seen above that the Reynolds number in the disc is expected to be very high, but this does not by itself imply that the disc is turbulent, unless there is an available energy source to keep the turbulence from decaying. In other words, we need to find some suitable instability able to extract energy from the rotational motion and keep the turbulence active.

The problem here is that purely hydrodynamic discs are expected to be linearly stable. In order to look for a stability condition, we consider standard perturbation theory and follow the evolution of a perturbation whose time and spatial dependence is in the form $\exp[i(\omega t - \mathbf{k} \cdot \mathbf{x})]$, where ω is the oscillation frequency and \mathbf{k} is the wavenumber. If ω has a negative imaginary part, the perturbation grows exponentially and instability occurs. The evolution of the perturbation can be obtained from the dispersion relation, which gives an expression for ω . For an incompressible, purely hydrodynamic rotating shear flow, the dispersion relation reads:

$$\omega^2 = \kappa^2, \quad (72)$$

where κ is the epicyclic frequency, given by:

$$\kappa^2 = \frac{2\Omega}{R} \frac{d(\Omega R^2)}{dR}, \quad (73)$$

and instability occurs whenever $\kappa^2 < 0$ (this is the well-known Rayleigh criterion for instability)³. Now, κ^2 is proportional to the radial derivative of the specific angular momentum, and in most astrophysical discs this is an increasing function of radius (in particular, for Keplerian discs, $\Omega R^2 \propto R^{1/2}$). This therefore means that purely hydrodynamic discs are generally linearly stable. As such they

³ Note that for a Keplerian disc the epicyclic frequency $\kappa = \Omega$.

are generally not thought to be able to provide a sustained source of energy to power turbulence and transport.

Even if the disc is linearly stable, it might turn out to be non-linearly unstable. Here, the situation is more complicated and the debate is still ongoing. Several authors have considered the generation and transport properties of vortices in discs (Godon and Livio, 2000; Klahr and Bodenheimer, 2003; Umurhan and Regev, 2004; Johnson and Gammie, 2005) but the general result is that while it is possible to induce substantial transport through vortices, this generally decays with time.

8.6. The magneto-rotational instability

The situation however changes drastically in the case in which the disc is threaded by a small magnetic field. In this case, a new instability, called the magneto-rotational instability (MRI), can arise (Balbus and Hawley, 1991). Several reviews have been recently dedicated to the MRI (Balbus and Hawley, 1998; Balbus, 2003) and it will be treated more extensively in the Chapter by Ferreira. Here, I will only briefly summarize its most salient features.

Despite being originally described in the late '50s (Velikhov, 1959; Chandrasekhar, 1960, 1961), this fundamental instability relevant to virtually any rotating shear flow under the effect of a magnetic field had never been considered as a possible source of transport in accretion discs until the '90s, when it was numerically shown by Hawley and Balbus (1991) that it could lead to significant transport in accretion discs, in the weak field case. Actually, the final confirmation of the importance of this instability only came a few years later, when it was shown by Hawley et al. (1995) that the same instability could lead to a non-decaying turbulence, with an associated non-vanishing stress.

A simple interpretation of the MRI is as follows. Consider the situation shown in Fig. 10. If dissipative effects are negligible (for example, if the fluid has no resistivity), the magnetic field lines are ‘frozen’ into the fluid, in the sense that along the motion of a fluid element, threaded by a magnetic field line, the field line stays attached to the element and is carried along by the flow. Now, consider two fluid elements (A and B) orbiting in the disc at the same radius and connected by a magnetic field line. Displace slightly the two elements in the radial direction (bottom of Fig. 10). Due to differential rota-

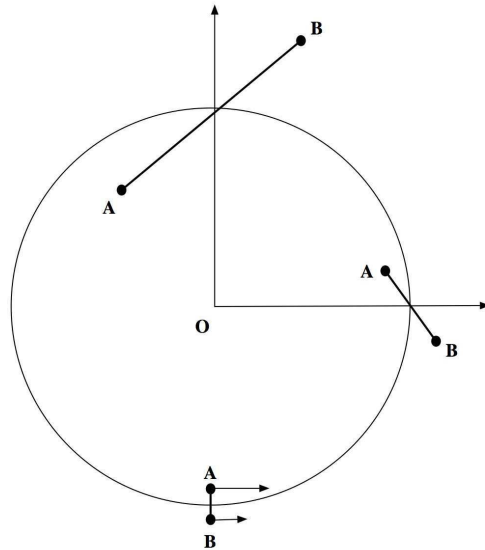


Fig. 10. Sketch illustrating the geometry leading to the MRI. Two fluid elements A and B are connected by a magnetic field line. Due to differential rotation, the field line stretches and magnetic tension leads to a transfer of angular momentum from A to B , causing A to sink down to the center and B to move outwards, further stretching the field line and thus leading to a runaway evolution.

tion, if $d\Omega/dR < 0$, A moves faster than B , so that after some time (right in Fig. 10) the field line will have been significantly stretched. A stretched field line provides a magnetic tension which slows down A (removing angular momentum) and accelerates B (giving angular momentum). Angular momentum is thus transferred from A to B so that A moves closer in while B moves outwards (top of Fig. 10), further stretching the field line and giving rise to a runaway process.

The stability of an MHD cylindrical flow was first considered by Velikhov (1959). Later, Chandrasekhar (1960) (see also Chandrasekhar 1961) obtained the dispersion relation for a differentially rotating flow threaded by a vertical magnetic field. The Chandrasekhar (1960) dispersion relation is (cf. the equivalent equation (79) in Balbus 2003):

$$\tilde{\omega}^4 - \tilde{\omega}^2 \kappa^2 - 4\Omega^2 (\mathbf{k} \cdot \mathbf{u}_A)^2 = 0, \quad (74)$$

where \mathbf{u}_A is the Alfvén velocity, \mathbf{k} is the wave-number of the perturbation and $\tilde{\omega}^2 = \omega^2 - (\mathbf{k} \cdot \mathbf{u}_A)^2$. Equation (74) can be easily solved for $\tilde{\omega}^2$, from which we can get ω^2 . A little algebra then shows that the disc is unstable (i.e., $\omega^2 < 0$) whenever:

$$(\mathbf{k} \cdot \mathbf{u}_A)^2 + \frac{d\Omega^2}{d \ln R} < 0. \quad (75)$$

The interesting thing here is that if we take the limit of vanishing magnetic field ($\mathbf{u}_A \rightarrow 0$) we do not recover the Rayleigh criterion for instability, but rather:

$$\frac{d\Omega^2}{d \ln R} < 0, \quad (76)$$

which (unlike the Rayleigh criterion) is generally satisfied by most astrophysically relevant discs.

Another interesting thing is that for any given magnetic field strength, short wavelength perturbations (with correspondingly large wavenumber) can be stabilized. Indeed, if λ is the wavelength, Eq. (75) implies that if

$$u_A^2 \gtrsim \Omega^2 \lambda^2 \quad (77)$$

the fluid would be stabilized. This is why the MRI is generally considered a weak field (or a large wavelength) instability. Since the largest wavelength that can fit in a disc is $H = c_s/\Omega$ (if we assume that turbulence develops isotropically), we then get that a supersonic magnetic field, for which $u_A > c_s$, is able to stabilize the flow against the MRI.

While this kind of instability is naturally applicable to accretion around compact objects, where the accretion flow is hot, some problems might arise for cold protoplanetary discs, where the ionization level is low (Fromang et al., 2002). Indeed, in this case, dissipative effects become important and the magnetic field becomes less coupled to the hydrodynamics of the disc. In this case, ‘dead zones’ are expected to develop, where the MRI is not active and accretion would be shut down. Actually, it has been shown by Gammie (1996) that cosmic rays can ionize the upper layers of the disc, thus leading to a so-called ‘layered disc’ where active accretion only occurs on the uppermost layers while the bulk of the disc stays inactive. However, Fleming and Stone (2003) show that even in a layered disc, velocity fluctuations in the active layers might induce a stress also in the bulk of the disc.

In the context of young stellar objects, models of discs where the transport is dominated by turbulence induced by the MRI have been developed throughout the years by, for example, Steinacker and Papaloizou (2002), Papaloizou and Nelson (2003) and Nelson and Papaloizou (2003).

8.7. Gravitational instability

Gravitational instabilities are sometimes considered unlikely to provide a significant source of angular momentum transport in discs, mainly because it is thought that only very massive discs would be self-gravitating. In fact, as shown in Section 4.4, in order to give a sizable contribution to the vertical gravitational field, the disc mass only needs to be a fraction $\sim H/R$ of the central object mass, which means that if the disc is thin, even a relatively low mass disc can display some effects connected to self-gravity. As we will show below, it is for disc masses of the same order of magnitude that gravitational instabilities develop. Now, if we take $H/R \approx 0.1$ and a central star of mass $M \approx 0.3M_\odot$, we then find that even a disc with a mass as low as $M_{\text{disc}} \approx 0.03M_\odot$ can be subject to gravitational instabilities⁴. Now, such disc masses are not uncommon (Eisner and Carpenter, 2006) and they would be quite likely especially at the earliest stages of star formation, where the mass balance of the protostar-disc system is more in favour of the disc. Clearly, as accretion proceeds and the disc mass becomes smaller, the effects of self-gravity would eventually die away. In any case, the importance of self-gravity in providing an effective way of redistributing angular momentum at the earliest stages of star formation has been recently clearly recognized (Hartmann et al., 2006).

Most of the recent interest in the dynamics of self-gravitating discs is also due to the fact that it can potentially lead to disc fragmentation and so produce low mass companions to young stars. A model for giant planet formation based on disc fragmentation has been put forward especially by Boss (2000) (see also Boss 2006; Mayer et al. 2002; Cai et al. 2006; Mayer et al. 2007). It turns out that the possibility of disc fragmentation due to gravitational instability depends strongly on the cooling rate of the disc, as I will discuss below, and therefore most of the research in this field aims at obtaining realistic estimates of the cooling processes in the disc. A recent review focusing on this particular aspect can be found in Durisen et al. (2007). Here, we will put instead more emphasis on the role of self-gravity in providing a source of transport to power the accre-

⁴ Note that in the case of accretion discs in Active Galactic Nuclei the aspect ratio is much smaller, $H/R \approx 10^{-3}$, so that discs with even lower masses relative to their central object are gravitationally unstable.

tion process (a thorough discussion of these aspects can also be found in Lodato 2008).

Gravitational instability in a disc is essentially a small modification of the standard Jeans instability in a three-dimensional homogeneous fluid. In the standard Jeans stability analysis, the natural tendency for collapse associated with self-gravity is balanced by pressure gradients. Now, pressure gradients are particularly effective at small wavelengths and tend to vanish for very large wavelengths. It is therefore not surprising that a system becomes Jeans unstable if it has a size larger than a fundamental lengthscale, called the Jeans length (that we have already encountered in Section 2).

In the case of a rotating disc, the situation gets more complicated not only because of the different geometry, but especially because the disc rotation provides another stabilizing effect, which in this case is more effective at large wavelengths. The combination of a short wavelength stabilization factor (pressure) and a large wavelength one (rotation) makes it possible, under appropriate conditions, to render the disc stable at all wavelengths. This is clearly seen when one considers the dispersion relation for tightly wound axi-symmetric disturbances in an infinitesimally thin, rotating disc (cf. Toomre 1964 in the case of a stellar disc, see also Binney & Tremaine 1987 and Bertin 2000 for the fluid case):

$$\omega^2 = c_s^2 k^2 - 2\pi G \Sigma |k| + \kappa^2, \quad (78)$$

where, as above, ω and k are the perturbation frequency and wavenumber and κ is the epicyclic frequency. In Eq. (78), the first term on the right hand side corresponds to the stabilizing effect of pressure, the second is the de-stabilizing effect of self-gravity, while the third is the stabilizing effect of rotation. Eq. (78) is a simple quadratic equation in k and it is straightforward to see that $\omega^2 < 0$ if and only if:

$$Q = \frac{c_s \kappa}{\pi G \Sigma} < 1. \quad (79)$$

Thus, the dimensionless parameter Q plays an important role in determining whether a gaseous disc is gravitationally unstable or not. We can now ask how massive should the disc be in order to be gravitationally unstable. This is easily derived from Eq. (79) in the case where $M_{\text{disc}} \ll M$:

$$Q \approx \frac{c_s \Omega}{\pi G \Sigma} = \frac{c_s}{\Omega R} \frac{GM}{\pi G \Sigma R^2} \approx \frac{H}{R} \frac{M}{M_{\text{disc}}(R)}, \quad (80)$$

which then shows that, as anticipated, in order for $Q \sim 1$, we should require that $(M_{\text{disc}}/M) \sim (H/R)$.

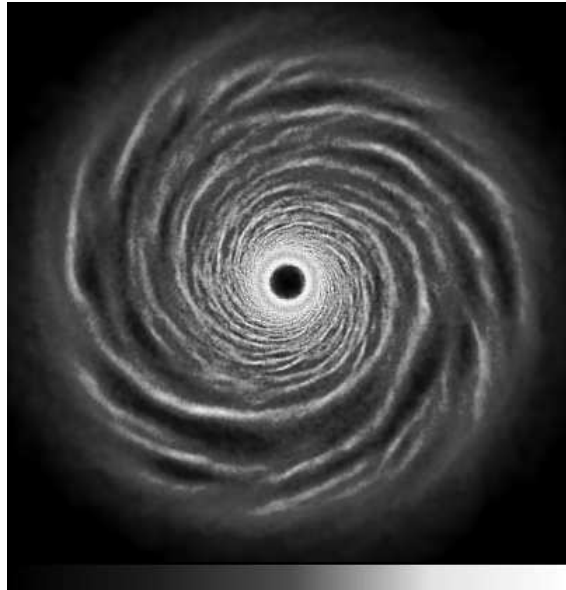


Fig. 11. Surface density of a self-regulated self-gravitating disc. In this case the mass ratio between the disc and the star was $M_{\text{disc}}/M = 0.1$. From Rice et al. (2005).

As we have seen above, disc masses of this order of magnitude might not be uncommon and it is therefore likely that young circumstellar discs are gravitationally unstable.

Having established that self-gravitating discs are linearly unstable, we should now ask what is the non-linear evolution of the instability and whether it can lead to a sustained transport of angular momentum. The stability criterion, Eq. (79) offers a natural way to describe this. Indeed, we should note that the stability parameter Q is proportional to the sound speed (and hence to temperature), so that colder discs are more unstable. Now, let us consider a disc which is initially hot, so that $Q \gg 1$ and the disc is stable. In the absence of other transport mechanisms (and neglecting stellar heating), the disc cools down due to radiative cooling until eventually $Q \approx 1$. At this stage, the disc develops a gravitational instability in the form of a spiral structure, that leads to angular momentum transport, and ultimately to energy dissipation and heating. In turn, the stability condition works like a kind of ‘thermostat’, so that heating turns on only if the disc is colder than a given temperature. If the ‘thermostat’ works, we should then expect the instability to self-regulate in such a way that the disc is always kept close to marginal stability, and thus a self-gravitating disc will evolve to a state where $Q \approx \bar{Q}$, where \bar{Q} is a constant of order unity (physical pro-

cesses of this kind also operate in the the dynamics of spiral galaxies, Bertin and Lin 1996). Analytical models of such self-regulated discs have been constructed and described by Bertin (1997), Bertin and Lodato (1999) and Lodato and Bertin (2003). The effectiveness of such a self-regulation mechanism has been shown (at least for relatively light discs, with $M_{\text{disc}}/M \lesssim 0.1$) by Lodato and Rice (2004, 2005), who have performed global hydrodynamical simulations of self-gravitating discs in the presence of cooling. These simulations indeed show that after an initial transient the disc settles down in a quasi-steady state, characterised by the presence of a spiral structure (to provide a source of transport and heating), and which only evolves secularly, on the viscous timescale. Fig. 11 shows a snapshot of one such simulation, where the spiral structure is clearly visible. In such quasi-steady state, the radial profile of Q is indeed found to be remarkably constant and close to unity.

What about the transport induced by gravitational instabilities? Here the very important point to remember is that this is strongly dependent on the effective cooling rate. This is a simple consequence of the self-regulation process described above. For a given cooling rate, the disc will try and provide (through the development of gravitational instabilities) a balancing heating term, otherwise the disc would cool down further and become more unstable, thus increasing the amplitude of the perturbation and the resulting stress and energy dissipation. Thus, once in a self-regulated state, not only does the temperature of the disc settle to a value such that $Q \approx 1$, but also the amplitude of the spiral structure induced by gravitational instability has to provide a stress large enough to balance the external cooling rate. Of course, in order to reproduce such behaviour in numerical simulations, as one might expect, one should go beyond a simple isothermal equation of state, as done in the pioneering work of Laughlin and Bodenheimer (1994). The importance of thermodynamics in the development of gravitational instabilities was first noted in the simulations by Pickett et al. (1998) and Pickett et al. (2000). However, it was not until Gammie (2001) that the connection described above was made explicit. Actually, we can also make a further step forward if we assume that the transport induced by gravitational instabilities can be described in terms of a ‘local’ viscosity (i.e. if we neglect possible non-local energy transport, that might in principle occur, see Balbus and Papaloizou 1999 and discussion in sec-

tion 8.3 above). In this case, the thermal timescale in the disc is closely related to the viscosity parameter α through the requirement of thermal equilibrium (Eq. (59)). In thermal equilibrium the thermal timescale is equal to the cooling timescale t_{cool} , and we therefore have:

$$\alpha = \frac{4}{9\gamma(\gamma - 1)} \frac{1}{t_{\text{cool}}\Omega}. \quad (81)$$

The strength of the torque induced by gravitational instabilities has been measured from numerical simulations in several papers (Gammie, 2001; Lodato and Rice, 2004, 2005; Mejia et al., 2005; Boley et al., 2006) and the relation described in Eq. (81) above has been confirmed both in cases where $t_{\text{cool}}\Omega$ is a constant (Gammie, 2001; Lodato and Rice, 2004) and in cases where it is not (Boley et al., 2006). This is also a confirmation that, at least in the cases considered in these papers (with some exceptions, see below), the transport induced by gravitational instabilities can be relatively well described in terms of a ‘local’ process.

From the discussion above, it would then appear that in principle it can be possible to produce through gravitational instabilities a stress with an effective α much larger than unity. This would be the value predicted by equation (81) for $t_{\text{cool}} \ll t_{\text{dyn}} = \Omega^{-1}$. Actually, it turns out that this is not the case. Gammie (2001) has shown that if $t_{\text{cool}} \lesssim 3\Omega^{-1}$, the disc, rather than achieving the above-mentioned self-regulated state, undergoes fragmentation. Rice et al. (2005) (see also Clarke et al. 2007) have later shown that the actual fragmentation boundary is dependent on the ratio of specific heats γ and ranges between $t_{\text{cool}} = 6\Omega^{-1}$ and $t_{\text{cool}} = 13\Omega^{-1}$. Also this behaviour is easily understood. Indeed, the growth rate of the instability is of the order of the dynamical timescale, and therefore for cooling times shorter than that, the disc has no time to develop the instability and reach thermal equilibrium, and collapse becomes inevitable. The dependency of the fragmentation threshold on γ found by Rice et al. (2005) offers another interpretation of the same phenomenon. It turns out, that for any value of γ the fragmentation boundary always occurs at the same value of $\alpha \approx 0.06$. It thus appear that gravitational instabilities in a steady state cannot provide a stress larger than $\alpha \approx 0.06$. If a larger stress is required in order to reach thermal equilibrium, then the disc will fragment.

The natural question at this stage is whether the cooling time in real discs is fast enough to allow frag-

mentation. This would then lead to a possible route to the formation of massive planets or low-mass stellar companions around a young star. Unfortunately, it turns out that, for realistic estimates (Rafikov, 2005) the cooling timescale is far too large, except possibly in the outer disc, at distances of the order of 100 AU from the star. This would then preclude the formation of giant planets through disc fragmentation, but would possibly allow for the formation of low-mass companions (in the brown dwarf mass range) at large separations (Lodato et al., 2005; Stamatellos et al., 2007). However, the issue of what is the cooling timescale in discs around young stars is not yet settled. The role of convection in the process has been sometimes discussed (see Boss 2004 and Rafikov 2007 for opposite views). Simulations which use a more realistic opacity prescription seem to result in an enhanced tendency for fragmentation (Johnson and Gammie, 2003) and certainly a detailed description of the evolution of the instability in the presence of strongly temperature dependent cooling is still lacking. Additionally, it has been sometimes suggested that the effect of an impulsive interaction with a stellar companion might induce fragmentation in massive discs (Boffin et al., 1998; Boss, 2006), but recent simulations tend to show the opposite result (Mayer et al., 2005; Lodato et al., 2007).

Before concluding, let us spend a few more words on the issue of locality, also in connection with the limiting values for the effective α provided by gravitational instabilities described above. It is well known from studies of the dynamics of spiral galaxies that if a disc is massive, then it will rapidly develop violent, bar-like instabilities (Ostriker and Peebles, 1973; Shlosman et al., 1989). Clearly such behaviour is not at all local and the transport associated with it can be much faster than viscous. However, most of the global simulations described above (performed by different groups with different numerical schemes) have not shown the development of a strong large-scale coherent structure. This is due to the fact that these simulations usually have focussed on relatively low mass discs (with $M_{\text{disc}}/M_{\star} \lesssim 0.1$). Actually, some of the numerical investigations mentioned above (Lodato and Rice, 2004, 2005) did reveal a change in behaviour when moving from light to massive discs, indicating an increasing role of global effects. First of all, the typical wavelength of the spiral structure appears to increase with increasing disc mass, and for disc masses $M_{\text{disc}}/M \gtrsim 0.1 - 0.2$ it can become compa-

rable with radius, clearly indicating that the local description would break down (Lodato and Rice, 2004). Indeed, such massive discs appear to be unable to reach a quasi-steady self-regulated state, even for relatively long cooling time. In this case, the disc is subject to large-scale, global instabilities (but not in the form of a bar), which show a highly variable temporal behaviour, and can lead to momentarily high values of α (in excess of the limiting values found for light discs). Such bursts of enhanced activity are recurrent and only last for timescales of the order of the dynamical time before decaying (and have sometimes been considered as a possible cause of FU Orionis outbursts, Vorobyov and Basu 2005). During such episodes, the disc is not in thermal equilibrium and it is not possible to compare the stress to the expectations based on a viscous model. Whether global energy transport does occur in these cases has not yet been investigated.

9. Challenges for the future

As we have seen above, studies of accretion disc dynamics have made significant progress since the early seminal investigations by Shakura and Sunyaev (1973) and Lynden-Bell and Pringle (1974). In particular, the increased computing power in the last fifteen years has made it possible to run numerical simulations of accretion discs, with ever increasing complexity. While until the '80s the origin of angular momentum transport in accretion discs was only discussed qualitatively, we now have the means to explore this issue quantitatively and to give more precise estimates of the magnitude of the internal disc stress. However, many issues still remain unresolved.

For example, as we have seen above, the interpretation of FU Orionis objects in terms of a limit cycle instability still faces some difficulties and to date no alternative theory has been fully developed. It is worth noting here the extreme importance of such objects in the context of investigating accretion on to young stars. FU Orionis objects are essentially the only objects whose emission is clearly dominated by accretion and which show a significant time evolution. As such, they are an ideal laboratory to study the accretion process and to place constraints on the magnitude of disc viscosity (analogously to the case of dwarf novae in the galactic binary case).

At a more fundamental level, while we can now

state with confidence that MHD instabilities, and in particular the MRI, plays an important role in determining the disc viscosity, numerical simulations have not reached a conclusive answer to what could be its magnitude. As pointed out by King et al. (2007), observational evidences from dwarf novae indicate that $\alpha \approx 0.1$, while most numerical simulations tend to get values which are at least one order of magnitude smaller. The numerical results appear to depend significantly on the geometry and on the magnitude of the imposed net magnetic field, and have probably not reached numerical convergence. In particular, it is difficult to model accurately very thin discs, while resolving fully the vertical structure, and in many cases simulations are only performed in a local “shearing box” approximation, which prevents the development of large scale perturbations. While it is true that observations of discs around young stars seem to imply smaller values of α with respect to the dwarf novae case, here we also have to take into account the additional complexity resulting from non-ideal MHD, since dissipative effects in the colder circumstellar discs are likely to reduce the effectiveness of the MRI.

We have seen above the large uncertainties on the non-linear outcome of gravitational instabilities. In this context, it is the thermodynamics of the discs that plays a major role in setting the saturation amplitude of the instability and therefore most studies are now concentrating on providing accurate estimates of the cooling rates, and the goal is eventually to be able to run reliable radiative transfer hydrodynamics simulations.

Finally, most theoretical studies on transport in accretion discs have focussed on ‘planar’ discs, so that the whole disc lies in the same plane. On the other hand, interactions with companion stars can easily induce a relatively large warp in the disc and such warped discs are often observed (Chiang and Murray-Clay, 2004; Akeson et al., 2007). Now, disc warping can provide significant dissipation and transport of angular momentum (Papaloizou and Pringle, 1983; Pringle, 1992; Lodato and Pringle, 2007) and such effects have been investigated only rarely (Larwood et al., 1996; Larwood and Papaloizou, 1997). The study of such non-planar discs is still a vast and largely unexplored territory.

Acknowledgements

I would like to thank Cathie Clarke and Jim Pringle for interesting discussions, Andrew King and Peter Cossins for a careful reading of the manuscript, Matthew Bate for providing Fig. 1 and Patrick Deegan and Graham Wynn for providing Fig. 8.

References

- F. C. Adams and F. H. Shu. *ApJ*, 308:836, 1986.
- F. C. Adams, C. J. Lada, and F. H. Shu. *ApJ*, 326: 865, 1988.
- R. L. Akeson, W. K. M. Rice, A. F. Boden, A. I. Sargent, J. M. Carpenter, and G. Bryden. *ArXiv e-prints*, 708, 2007.
- R. D. Alexander and P. J. Armitage. *ApJ*, 639:L83, 2006.
- S. M. Andrews and J. P. Williams. *ApJ*, 631:1134, 2005.
- S. M. Andrews and J. P. Williams. *ApJ*, 659:705, 2007.
- P. J. Armitage. *ArXiv e-prints: 0701485*, 2007.
- P. J. Armitage, M. Livio, and J. E. Pringle. *MNRAS*, 324:705, 2001.
- S. A. Balbus. *ARA&A*, 41:555, 2003.
- S. A. Balbus and J. F. Hawley. *ApJ*, 376:214, 1991.
- S. A. Balbus and J. F. Hawley. *Reviews of Modern Physics*, 70:1, 1998.
- S. A. Balbus and J. C. B. Papaloizou. *ApJ*, 521:650, 1999.
- M. R. Bate, I. A. Bonnell, and V. Bromm. *MNRAS*, 339:577, 2003.
- S. V. W. Beckwith, A. I. Sargent, R. S. Chini, and R. Guesten. *AJ*, 99:924, March 1990.
- C. A. Beichman, P. C. Myers, J. P. Emerson, S. Harris, R. Mathieu, P. J. Benson, and R. E. Jennings. *ApJ*, 307:337, 1986.
- K. R. Bell and D. N. C. Lin. *ApJ*, 427:987, 1994.
- K. R. Bell, D. N. C. Lin, L. W. Hartmann, and S. J. Kenyon. *ApJ*, 444:376, 1995.
- G. Bertin and C. C. Lin. *Spiral Structure in Galaxies: a Density Wave Theory*. MIT Press, Cambridge, 1996.
- G. Bertin. *ApJ*, 478:L71, 1997.
- G. Bertin. *Dynamics of Galaxies*. Cambridge University Press, Cambridge, 2000.
- G. Bertin and G. Lodato. *A&A*, 350:694, 1999.
- Binney, J., & Tremaine, S. *Galactic Dynamics*. Princeton, NJ, Princeton University Press, 1987,

- H. M. J. Boffin, S. J. Watkins, A. S. Bhattal, N. Francis, and A. P. Whitworth. *MNRAS*, 300:1189, 1998.
- A. C. Boley, A. C. Mejía, R. H. Durisen, K. Cai, M. K. Pickett, and P. D'Alessio. *ApJ*, 651:517, 2006.
- I. Bonnell and P. Bastien. *ApJ*, 401:31, 1992.
- A. P. Boss. *ApJ*, 536:L101, 2000.
- A. P. Boss. *ApJ*, 610:456, 2004.
- A. P. Boss. *ApJ*, 641:1148, 2006.
- K. Cai, R. H. Durisen, S. Michael, A. C. Boley, A. C. Mejía, M. K. Pickett, and P. D'Alessio. *ApJ*, 636:L149, 2006.
- R. Cesaroni, D. Galli, G. Lodato, C. M. Walmsley, and Q. Zhang. In B. Reipurth, D. Jewitt, and K. Keil, editors, *Protostars and Planets V*, page 197, 2007.
- S. Chandrasekhar. *Hydrodynamic and hydromagnetic Stability*. Clarendon Press, Oxford, 1961.
- S. Chandrasekhar. *Proceedings of the National Academy of Sciences*, 46:53, 1960.
- E. I. Chiang and R. A. Murray-Clay. *ApJ*, 607:913, 2004.
- E. P. Chiang and P. Goldreich. *ApJ*, 490:368, 1997.
- C. Clarke, G. Lodato, S. Y. Melnikov, and M. A. Ibrahimov. *MNRAS*, 361:942, 2005.
- C. Clarke, E. Harper-Clark, and G. Lodato. *ArXiv e-prints*, 708, 2007.
- C. J. Clarke and P. J. Armitage. *MNRAS*, 345:691, 2003.
- C. J. Clarke and J. E. Pringle. *MNRAS*, 351:1187, 2004.
- C. J. Clarke and J. E. Pringle. *MNRAS*, 370:L10, 2006.
- C. J. Clarke and D. Syer. *MNRAS*, 278:L23, 1996.
- C. J. Clarke, D. N. C. Lin, and J. C. B. Papaloizou. *MNRAS*, 236:495, 1989.
- C. J. Clarke, D. N. C. Lin, and J. E. Pringle. *MNRAS*, 242:439, 1990.
- C. P. Dullemond, C. Dominik, and A. Natta. *ApJ*, 560:957, 2001.
- C. P. Dullemond, D. Hollenbach, I. Kamp, and P. D'Alessio. *Protostars and Planets V*, page 555, 2007.
- R. H. Durisen, A. P. Boss, L. Mayer, A. F. Nelson, T. Quinn, and W. K. M. Rice. In B. Reipurth, D. Jewitt, and K. Keil, editors, *Protostars and Planets V*, page 607, 2007.
- A. Dutrey et al. *A&A*, 309:493, 1996.
- J. A. Eisner and J. M. Carpenter. *ApJ*, 641:1162, 2006.
- J. A. Eisner, L. A. Hillenbrand, J. M. Carpenter, and S. Wolf. *ApJ*, 635:396, 2005.
- J. Faulkner, D. N. C. Lin, and J. Papaloizou. *MNRAS*, 205:359, 1983.
- T. Fleming and J. M. Stone. *ApJ*, 585:908, 2003.
- J. Frank, A. King, and D. Raine. *Accretion Power in Astrophysics*. Cambridge University Press, Cambridge, 2002.
- S. Fromang, C. Terquem, and S. A. Balbus. *MNRAS*, 329:18, 2002.
- C. F. Gammie. *ApJ*, 553:174, 2001.
- C. F. Gammie. *ApJ*, 457:355, 1996.
- P. Godon and M. Livio. *ApJ*, 537:396, 2000.
- E. Gullbring, L. Hartmann, C. Briceño, and N. Calvet. *ApJ*, 492:323, 1998.
- E. Gullbring, N. Calvet, J. Muzerolle, and L. Hartmann. *ApJ*, 544:927, 2000.
- K.E. Haisch, E.A. Lada, and C.J. Lada. *ApJ*, 552:L153, 2001.
- L. Hartmann. *Accretion Processes in Star Formation*. Cambridge University Press, Cambridge, 1998.
- L. Hartmann and S. J. Kenyon. *ARA&A*, 34:207, 1996.
- L. Hartmann and S. J. Kenyon. *ApJ*, 299:462, 1985.
- L. Hartmann, N. Calvet, E. Gullbring, and P. D'Alessio. *ApJ*, 495:385, 1998.
- L. Hartmann, P. D'Alessio, N. Calvet, and J. Muzerolle. *ApJ*, 648:484, 2006.
- J. F. Hawley and S. A. Balbus. *ApJ*, 376:223, 1991.
- J. F. Hawley, C. F. Gammie, and S. A. Balbus. *ApJ*, 440:742, 1995.
- E. Hayashi and T. Matsuda. *Prog. Theor. Phys.*, 105:531, 2001.
- G. H. Herbig, P. P. Petrov, and R. Duemmler. *ApJ*, 595:384, 2003.
- H. Ji, M. Burin, E. Schartman, and J. Goodman. *Nature*, 444:343, 2006.
- B. M. Johnson and C. F. Gammie. *ApJ*, 597:131, 2003.
- B. M. Johnson and C. F. Gammie. *ApJ*, 635:149, 2005.
- S. J. Kenyon and L. Hartmann. *ApJ*, 323:714, 1987.
- S. J. Kenyon and L. Hartmann. *ApJ*, 383:664, 1991.
- S. J. Kenyon, L. Hartmann, and R. Hewett. *ApJ*, 325:231, February 1988. doi: 10.1086/165999.
- S. J. Kenyon, N. Calvet, and L. Hartmann. *ApJ*, 414:676, 1993.
- A. R. King. *MNRAS*, 296:L45, 1998.
- A. R. King, J. E. Pringle, and M. Livio. *MNRAS*, 376:1740, 2007.
- H. H. Klahr and P. Bodenheimer. *ApJ*, 582:869, 2003.

- C. J. Lada and B. A. Wilking. *ApJ*, 287:610, 1984.
- J. D. Larwood and J. C. B. Papaloizou. *MNRAS*, 285:288, 1997.
- J. D. Larwood, R. P. Nelson, J. C. B. Papaloizou, and C. Terquem. *MNRAS*, 282:597, 1996.
- Lasota, J.-P. *New Astronomy Review*, 45:449, 2001.
- G. Laughlin and P. Bodenheimer. *ApJ*, 436:335, 1994.
- G. Lesur and P.-Y. Longaretti. *A&A*, 444:25, 2005.
- D.N.C. Lin, J. Faulkner, and J. Papaloizou. *MNRAS*, 212:105, 1985.
- G. Lodato and G. Bertin. *A&A*, 408:1015, 2003.
- G. Lodato and C. J. Clarke. *MNRAS*, 353:841, 2004.
- G. Lodato and J. E. Pringle. *ArXiv e-prints*, 708, 2007.
- G. Lodato and W. K. M. Rice. *MNRAS*, 351:630, 2004.
- G. Lodato and W. K. M. Rice. *MNRAS*, 358:1489, 2005.
- G. Lodato, E. Delgado-Donate, and C. J. Clarke. *MNRAS*, 364:L91, 2005.
- G. Lodato, F. Meru, C. J. Clarke, and W. K. M. Rice. *MNRAS*, 374:590, 2007.
- G. Lodato. *Rivista del Nuovo Cimento*, 30:293, 2007. *In press*.
- R. Lüst. *Z. Naturforsch.*, 7a:87, 1952
- D. Lynden-Bell and A. J. Kalnajs. *MNRAS*, 157:1, 1972.
- D. Lynden-Bell and J. E. Pringle. *MNRAS*, 168:603, 1974.
- Machida, M. N., Tomisaka, K., & Matsumoto, T. 2004, *MNRAS*, 348, L1
- F. Malbet et al. *A&A*, 437:627, 2005.
- F. Malbet et al. *ApJ*, 507:L149, 1998.
- T. Matsuda and E. Hayashi. *Prog. Theor. Phys.*, 112:357, 2004.
- L. Mayer, J. Wadsley, T. Quinn, and J. Stadel. *MNRAS*, 363:641, 2005.
- L. Mayer, G. Lufkin, T. Quinn, and J. Wadsley. *ApJ*, 661:L77, May 2007.
- L. Mayer et al. *Science*, 298:1756, 2002.
- McKee, C. F., & Ostriker, E. C. 2007, *ARA&A*, 45, 565
- A. C. Mejia, R. H. Durisen, M. K. Pickett, and K. Cai. *ApJ*, 619:1098, 2005.
- R. Millan-Gabet et al. *ApJ*, 641:547, 2006.
- B. Mukhopadhyay, N. Afshordi, and R. Narayan. *ApJ*, 629:383, 2005.
- A. Natta, L. Testi, J. Muzerolle, S. Randich, F. Comerón, and P. Persi. *A&A*, 424:603, 2004.
- A. Natta, L. Testi, R. Neri, D. S. Shepherd, and D. J. Wilner. *A&A*, 416:179, 2004.
- R. P. Nelson and J. C. B. Papaloizou. *MNRAS*, 339:993, 2003.
- J. P. Ostriker and P. J. E. Peebles. *ApJ*, 186:467, 1973.
- J. Papaloizou, J. Faulkner, and D. N. C. Lin. *MNRAS*, 205:487, 1983.
- J. C. B. Papaloizou and R. P. Nelson. *MNRAS*, 339:983, 2003.
- J. C. B. Papaloizou and J. E. Pringle. *MNRAS*, 202:1181, 1983.
- M. E. Pessah, C.-k. Chan, and D. Psaltis. *ArXiv Astrophysics e-prints*, 2006.
- B. K. Pickett et al. *ApJ*, 529:1034, 2000.
- B. K. Pickett et al. *ApJ*, 504:468, 1998.
- R. Popham, R. Narayan, L. Hartmann, and S. J. Kenyon. *ApJ*, 415:L127, 1993.
- Price, D. J., & Bate, M. R. 2007, *MNRAS*, 377, 77
- J. E. Pringle. *ARA&A*, 19:137, 1981.
- J. E. Pringle. *MNRAS*, 258:811, 1992.
- R. Rafikov. *ApJ*, 621:69, 2005.
- R. R. Rafikov. *ApJ*, 662:642, 2007.
- W. K. M. Rice, G. Lodato, J. E. Pringle, P. J. Armitage, and I. A. Bonnell. *MNRAS*, 355:543, 2004.
- W. K. M. Rice, G. Lodato, and P. J. Armitage. *MNRAS*, 364:L56, 2005.
- W. K. M. Rice, G. Lodato, J. E. Pringle, P. J. Armitage, and I. A. Bonnell. *MNRAS*, 372:L9, 2006.
- D. Richard and J.-P. Zahn. *A&A*, 347:734, 1999.
- A. Scholz, R. Jayawardhana, and K. Wood. *ApJ*, 645:1498, 2006.
- N. I. Shakura and R. A. Sunyaev. *A&A*, 24:337, 1973.
- I. Shlosman, J. Frank, and M. C. Begelman. *Nature*, 338:45, March 1989.
- A. Sicilia-Aguilar et al. *ApJ*, 638:897, 2006.
- L. Spitzer. *ApJ*, 95:329, 1942.
- D. Stamatellos, D. Hubber, and A. Whitworth. *ArXiv e-prints*, 708, 2007.
- A. Steinacker and J. C. B. Papaloizou. *ApJ*, 571:413, 2002.
- L. Testi et al. *ApJ*, 554:1087, 2001.
- A. Toomre. *ApJ*, 139:1217, 1964.
- O. M. Umurhan and O. Regev. *A&A*, 427:855, 2004.
- E. P. Velikhov. *Soviet Physics - JETP*, 36:995, 1959.
- C. F. von Weizsäcker. *Z. Naturforsch.*, 3a:524, 1948
- E. I. Vorobyov and S. Basu. *ApJ*, 633:L137, 2005.
- E. I. Vorobyov and S. Basu. *ApJ*, 650:956, 2006.
- H. Wang, D. Apai, T. Henning, and I. Pascucci. *ApJ*, 601:L83, 2004.
- S.J. Weidenschilling. *MNRAS*, 180:57, 1977.